

Regge poles and high energy scattering

6.1 Introduction

Having identified, in the previous chapter, some of the leading Regge trajectories from the resonance spectrum, we next want to look more closely at the other main aspect of Regge theory, the way in which Regge poles in the crossed t channel control the high energy behaviour of scattering amplitudes in the direct s channel.

For spinless-particle scattering this presents few problems; we would simply use the expression (2.8.10) in the region where t is small and negative, and s is large. However, for real experiments with spinning particles it is a bit more difficult because, as we shall find in the next section, the t -channel helicity amplitudes contain various kinematical factors, and are subject to various constraints, which must also be incorporated in the Regge residues. Also we shall need to look closely at the behaviour of the residue function when a trajectory passes through the nonsense points discussed in section 4.5. Only when we have clarified these kinematical requirements can we write down correct expressions for the Regge pole contribution to a scattering amplitude based on (4.6.15).

In exploring these kinematical problems we shall discover that some of the difficulties at $t = 0$ may imply the occurrence of additional trajectories called 'daughters' and 'conspirators', and we shall briefly review the application of group theoretical techniques to such problems. Also we examine the way in which the internal SU(2) and SU(3) symmetries constrain Regge pole exchange models.

We are thus led to (6.8.1) below for the parameterization of a Reggeon exchange amplitude, and in the extended final section of this chapter we discuss the comparison of this expression with the experimental data on high energy scattering processes. A reader who is mainly interested in the phenomenology could start at section 6.8 and refer back as necessary.

6.2 Kinematical singularities of Regge residues*

We noted in section 4.1 that though helicity amplitudes have many advantages for Regge theory they suffer from the defect that they are not generally free of kinematical singularities. Since the residue of a t -channel Regge pole is given by (see (4.6.1) and cf. (3.2.16))

$$\beta_H(t) = \frac{1}{2\pi i} \oint dJ A_{HJ}^{\eta}(t) \quad (6.2.1)$$

the integration contour being taken round the pole at $J = \alpha(t)$, it is clear from our discussion in section 3.2 that $\beta_H(t)$ will inherit the singularities of $A_{HJ}^{\eta}(t)$, i.e. the kinematical singularities as well as the dynamical right-hand cut beginning at the t -channel threshold. But it will not, of course, contain the pole, nor, in view of the argument of section 3.2, the left-hand cut of $A_{HJ}^{\eta}(t)$.

Various methods have been devised for obtaining the kinematical singularities. One way is to make use of the relationship between helicity amplitudes and the invariant amplitudes of (4.1.3) which are free of kinematical singularities (Cohen-Tannoudji, Salin and Morel 1968), but this becomes difficult for high spins. Another technique, devised by Hara (1964), and worked out fully by Wang (1966), makes use of the fact that the only kinematical t -singularities of an s -channel helicity amplitude occur in the half-angle factors (4.4.12). And in view of the crossing relation (4.3.7) it is evident that the only kinematical singularities in t of the t -channel helicity amplitudes are either those of the s -channel amplitudes, or singularities which are present in the crossing matrix (4.3.4), which is known. A very complete account of this method is given in Martin and Spearman (1970, chapter 6).

But with both methods the physical reasons for the occurrence of the kinematical factors are rather obscure, and instead we shall employ a less rigorous method based on Jackson and Hite (1968) which makes the physics clearer.

The s -singularities of a t -channel helicity amplitude stem entirely from the half-angle factors of (4.4.16), and their occurrence is readily explained by the fact that angular-momentum conservation in the forward and backward directions requires the vanishing of helicity-flip amplitudes (see section 4.4). Similarly we shall find that the t kinematical factors, which for the processes $1 + \bar{3} \rightarrow \bar{2} + 4$ may occur at the thresholds $t = (m_1 + m_3)^2$ and $t = (m_2 + m_4)^2$, pseudo-thresholds

* This section may be omitted at first reading.

$t = (m_1 - m_3)^2$ and $t = (m_2 - m_4)^2$, or at $t = 0$, also have a simple physical explanation. We begin by assuming that $m_1 > m_3$ and $m_2 > m_4$, but will consider equal masses, for which the pseudo-threshold moves to $t = 0$, later.

We have found both in non-relativistic potential scattering, in (3.3.24), and for spinless particle scattering, in (2.6.8), that at the threshold $t = (m_1 + m_3)^2$ the partial-wave amplitude has the behaviour

$$A_l(t) \sim (q_{t13})^l \sim (T_{13}^+(t))^l \quad (6.2.2)$$

in the notation of (2.6.6), due to the opening of the partial-wave phase space. Since scattering near threshold is non-relativistic we may expect that even for particles which have spin the threshold behaviour will similarly be

$$A_{HJ}^{\eta}(t) \sim (T_{13}^+(t))^L \quad (6.2.3)$$

where L is the lowest value of l that can occur for the given J . This will generally be $L = J - \sigma_1 - \sigma_3$ (i.e. σ_1, σ_3 and l all parallel) unless this value of l has the wrong parity, in which case $L = J - (\sigma_1 + \sigma_3) + 1$. This may be incorporated in the expression

$$\left. \begin{aligned} L &= J - \sigma_1 - \sigma_3 + \frac{1}{2}[1 - \eta P_1 P_3 (-1)^{\sigma_1 + \sigma_3 - v}] \\ &\equiv J - Y_{13}^+ \quad (\text{say}) \end{aligned} \right\} \quad (6.2.4)$$

where P_1, P_3 ($= \pm 1$) are the intrinsic parities of the particles, and v is defined in (4.5.6).

We found in section 2.6 that the behaviour (6.2.2) is guaranteed for spinless particle scattering by the Froissart–Gribov projection (2.6.2) (where it converges). However, in (4.5.7) $e_{\lambda\lambda'}^J(z_t) \sim (T_{13}^+)^{J+1}$ (from (1.7.19) and (B.25)), $\xi_{\lambda\lambda'}(z_t) \sim (T_{13}^+)^{-M}$ (from (B.11)) where

$$M \equiv \max\{|\lambda|, |\lambda'|\}, \quad \text{and} \quad dz_t \sim ds(T_{13}^+)^{-1}$$

giving instead

$$A_{HJ}^{\eta}(t) \sim (T_{13}^+)^{J-M}, \quad t \rightarrow (m_1 + m_3)^2 \quad (6.2.5)$$

So the only way in which (6.2.3) can be obtained from (4.5.7) is if the extra factors are already present as kinematical factors in $A_{H_i}(s, t)$, and hence in $D_{sH}(s, t)$ etc. So we must have

$$A_{H_i}(s, t) \sim (T_{13}^+)^{M-Y_{13}^+} \quad \text{as} \quad t \rightarrow (m_1 + m_3)^2 \quad (6.2.6)$$

A similar result holds at the $\bar{24}$ threshold. But the pseudo-threshold corresponds to the threshold for a process in which the lighter particle (say m_3) has the rest energy $E = -m_3$. Such negative energy states (or 'holes') correspond to anti-particles, and for fermions (but not bosons)

the anti-particle has the opposite parity to its particle, so we must replace P_3 by $P_3(-1)^{2\sigma_3}$. So we end up with the threshold behaviour

$$A_{H_i}(s, t) \propto (T_{13}^+)^{M-Y_{13}^+} (T_{13}^-)^{M-Y_{13}^-} (T_{24}^-)^{M-Y_{24}^+} (T_{24}^+)^{M-Y_{24}^-} \tag{6.2.7}$$

where $Y_{ij}^\pm \equiv \sigma_i + \sigma_j - \frac{1}{2}[1 - \eta P_i P_j (-1)^{\sigma_i \pm \sigma_j - \nu}]$

for $m_i > m_j$. Of course if, say, $m_1 = m_3$, the pseudo-threshold moves to $t = 0$, while if $m_3 = m_4$ also both pseudo-thresholds will be at $t = 0$. These cases will be considered below. So after the partial-wave projection (4.5.7) has been performed, because of (6.2.5) we find

$$A_{HJ}^{\eta}(t) \propto \bar{K}_{\lambda\lambda'}(t)(q_{t13}q_{t24})^{J-M} \tag{6.2.8}$$

where $\bar{K}_{\lambda\lambda'}(t)$ is the kinematical factor defined in table 6.1 on p. 160, and so from (6.2.1)

$$\beta_H(t) = \bar{K}_{\lambda\lambda'}(t) \left(\frac{q_{t13}q_{t24}}{s_0} \right)^{\alpha(t)-M} \bar{\beta}_H(t) \tag{6.2.9}$$

where $\bar{\beta}_H(t)$ is free of kinematical singularities at the thresholds and pseudo-thresholds (but not necessarily at $t = 0$). We have introduced an arbitrary scale factor s_0 , with the same units as t , so that the units in which $\bar{\beta}_H$ is measured will not vary with $\alpha(t)$. It will be discussed further in section 6.8*a*.

There is an additional problem at the thresholds, however, that in general the various helicity amplitudes for a given process are not all independent (see Jackson and Hite 1968, Trueman 1968). This is because at threshold, in view of (6.2.2), only the $l = 0$ state survives, and, to keep $l = 0$, J is restricted to the range $|\sigma_1 - \sigma_3| \leq J \leq \sigma_1 + \sigma_3$, so only these values of J appear in the partial-wave series (4.4.14). So if we define $\mathbf{s} \equiv \sigma_1 + \sigma_3$ and expand our partial-wave helicity states $|J, \lambda; \lambda_1, \lambda_3\rangle$ ($\lambda \equiv \lambda_1 - \lambda_3$) in terms of $l - s$ states $|J, \lambda; l, s\rangle$, at threshold we find, since $l = 0, s = J$,

$$|J, \lambda; \lambda_1, \lambda_3\rangle = N_J \langle \sigma_1, \lambda_1, \sigma_3, \lambda_3 | J, \lambda \rangle |J, \lambda; 0, J\rangle \tag{6.2.10}$$

where N_J is a normalization factor and $\langle \sigma_1, \lambda_1, \sigma_3, \lambda_3 | J, \lambda \rangle$ is the Clebsch-Gordan coefficient. So at threshold a partial-wave helicity amplitude can be written in the form

$$A_{HJ}^{\eta}(t) = \langle \sigma_1, \lambda_1, \sigma_3, \lambda_3 | J, \lambda \rangle a_{\lambda_2\lambda_4}(J, t) \tag{6.2.11}$$

where $a_{\lambda_2\lambda_4}(J, t)$ is independent of λ_1 and λ_3 . So on summing over $J, |\sigma_1 - \sigma_3| \leq J \leq \sigma_1 + \sigma_3$, the various $A_{H_i}(s, t)$ with the same values of λ_2, λ_4 but different λ_1, λ_3 , are all related at the $1\bar{3}$ threshold by a sum over the Clebsch-Gordan coefficients appearing in (6.2.11).

This is best illustrated by an example. Thus if we consider elastic πN scattering for which the t -channel process is $\pi\pi \rightarrow N\bar{N}$ we find that at the $N\bar{N}$ threshold, $t = 4m_N^2$, the relation between the amplitudes of (4.3.11) reads

$$A_{++}(s, t) \rightarrow -iA_{+-}(s, t), \quad t \rightarrow 4m_N^2 \quad (6.2.12)$$

the factor $(-i)$ coming from the half-angle factor (see (6.2.15) below). Then if we take out all the kinematical factors we have (cf. (4.3.11))

$$\left. \begin{aligned} A_{++}(s, t) &= \hat{A}_{++}(s, t) (t - 4m_N^2)^{-\frac{1}{2}} \\ A_{+-}(s, t) &= \hat{A}_{+-}(s, t) t^{\frac{1}{2}} (t - 4m_N^2)^{\frac{1}{2}} (1 - z_t^2)^{\frac{1}{2}} \end{aligned} \right\} \quad (6.2.13)$$

where the \hat{A} 's are free of kinematical singularities in both s and t . If we express each of these amplitudes in terms of a single Regge pole $\alpha(t)$, we have (from (6.8.1) below)

$$\left. \begin{aligned} A_{++}(s, t) &= \gamma_1(t) (t - 4m_N^2)^{-\frac{1}{2}} \left(\frac{s}{s_0}\right)^{\alpha(t)} \\ A_{+-}(s, t) &= \gamma_2(t) t^{\frac{1}{2}} (t - 4m_N^2)^{\frac{1}{2}} (1 - z_t^2)^{\frac{1}{2}} \left(\frac{s}{s_0}\right)^{\alpha(t)-1} \end{aligned} \right\} \quad (6.2.14)$$

$$\xrightarrow{s \rightarrow \infty} i\gamma_2(t) t^{\frac{1}{2}} (t - 4m_N^2)^{-\frac{1}{2}} \left(\frac{s}{s_0}\right)^{\alpha(t)} \quad (6.2.15)$$

where the γ 's are kinematical-singularity-free residues. The relation (6.2.12) then becomes

$$\gamma_1(4m_N^2) = 2m_N \gamma_2(4m_N^2) \quad (6.2.16)$$

and we can always ensure that this will be satisfied by writing

$$2m_N \gamma_2(t) = \gamma_1(t) + \gamma_3(t) \left(\frac{4m_N^2 - t}{4m_N^2}\right) \quad (6.2.17)$$

where now $\gamma_1(t)$ and $\gamma_3(t)$ are free of constraints as well as singularities. Putting (6.2.14) and (6.2.15) in (4.3.12) gives

$$\frac{d\sigma}{dt} = \frac{1}{64\pi s q_{s12}^2} \frac{1}{4m_N^2} \left(\frac{s}{s_0}\right)^{2\alpha(t)} \left\{ \gamma_1^2(t) - \frac{t}{4m_N^2} \left[2\gamma_1(t) \gamma_3(t) + \gamma_3^2(t) \left(1 - \frac{t}{4m_N^2}\right) \right] \right\}. \quad (6.2.18)$$

This expression has no singularity at $t = 4m_N^2$, but had we used (6.2.14) and (6.2.15) directly, ignoring the constraint (6.2.16), there would have been a spurious pole at this point.

This is a rather cumbersome procedure, and it is therefore fortunate that usually the thresholds are sufficiently far from the s -channel physical region ($t < 0$) for it not to matter much in practice if we

ignore the constraint. It is only really important in cases like $\pi N \rightarrow \pi \Delta$ where the pseudo-threshold at $t = (m_\Delta - m_N)^2$ is not so far from $t = 0$.

We must next consider the point $t = 0$. If the masses are unequal, i.e. $m_1 \neq m_3, m_2 \neq m_4$, then from (1.7.19)

$$z_t \xrightarrow[t \rightarrow \infty]{} \epsilon \equiv \pm 1 \quad \text{for} \quad (m_1 - m_3)(m_2 - m_4) \geq 0 \quad (6.2.19)$$

So the half-angle factor (4.4.12) has the behaviour

$$\xi_{\lambda\lambda'}(z_t) \underset{t \rightarrow 0}{\sim} t^{\frac{1}{2}|\lambda - \epsilon\lambda'|} \quad (6.2.20)$$

and so from (4.4.16) $\hat{A}_{H_t}(s, t) \sim t^{-\frac{1}{2}|\lambda - \epsilon\lambda'|}$ (6.2.21)

Hence the definite parity amplitudes (4.6.10) have the behaviour

$$\hat{A}_{H_t}^\eta(s, t) \sim t^{-\frac{1}{2}|\lambda - \epsilon\lambda'|} a_1(s, t) \pm \eta t^{-\frac{1}{2}|\lambda + \epsilon\lambda'|} a_2(s, t) \quad (6.2.22)$$

where a_1 and a_2 are regular at $t = 0$. So $\hat{A}_{H_t}^\eta$ has a singularity of the form

$$\hat{A}_{H_t}^\eta(s, t) \sim \frac{a^\eta}{t^{\frac{1}{2} \max\{|\lambda + \lambda'|, |\lambda - \lambda'|\}}} = \frac{a^\eta}{t^{\frac{1}{2}(M+N)}} \quad (6.2.23)$$

where a^η is one of a_1, a_2 and M, N are defined in (4.4.15), (4.5.11). But a Regge pole, which has a definite parity, cannot have such a singular behaviour as this, because if it did we would find

$$A_{H_t}(s, t) \equiv \xi_{\lambda\lambda'}(z_t) \hat{A}_{H_t}(s, t) \underset{t \rightarrow 0}{\sim} t^{\frac{1}{2}|\lambda - \epsilon\lambda'|} \frac{1}{2} (a^\eta t^{-\frac{1}{2}(M+N)} \mp \eta a^{-\eta} t^{-\frac{1}{2}(M+N)}) \quad (6.2.24)$$

(where $-\eta = (-1)\eta$) which is singular unless $a^\eta = \pm \eta a^{-\eta}$, except when $\lambda = \lambda' = 0$. This equality of a^η and $a^{-\eta}$ in fact follows directly from (6.2.22), (6.2.23), but obviously it cannot be satisfied by a Regge pole with a definite parity. So instead of (6.2.23) we must choose the less singular behaviour

$$\hat{A}_{H_t}^\eta(s, t) \sim \frac{a^\eta}{t^{\frac{1}{2} \min\{|\lambda + \lambda'|, |\lambda - \lambda'|\}}} = \frac{a^\eta}{t^{\frac{1}{2}(M-N)}} \quad (6.2.25)$$

i.e. we multiply (6.2.23) by t^N . (However, for channels with odd Fermion number N is a half-integer, so this would introduce a spurious square-root branch point – see section 6.5 for this case.)

To obtain the $t = 0$ behaviour of the residue from (6.2.25) we note that (6.2.9) has a singularity of the form $t^{-(\alpha(t)-M)}$ from (1.7.15). The $t^{-\alpha}$ will cancel with the corresponding singularity in the asymptotic behaviour of the rotation function in (4.6.4),

$$e_{\lambda\lambda'}^{-\alpha-1}(z_t) \sim \left(\frac{z_t}{2}\right)^\alpha \sim \left(\frac{s-u}{8q_{t13}q_{t24}}\right)^\alpha \quad (6.2.26)$$

from (B.25), but the t^M remains, so we end up with

$$\beta_H(t) = t^{-\frac{1}{2}(M+N)} \bar{K}_{\lambda\lambda'}(t) \left(\frac{q_{t13} q_{t24}}{s_0} \right)^{\alpha(t)-M} \bar{\gamma}_H(t) \tag{6.2.27}$$

where $\bar{\gamma}_H(t)$ is free of kinematical singularities. Unfortunately this will not do either, because its behaviour for $t \rightarrow 0$, $\beta_H(t) \sim t^{\frac{1}{2}(M-N)-\alpha}$, is not factorizable between the initial and final states. We must be able to write

$$\beta_H(t) = \beta_\lambda(t) \beta_{\lambda'}(t) \tag{6.2.28}$$

which is possible only if we change the $t = 0$ behaviour to $t^{\frac{1}{2}(M+N)-\alpha}$, so we finally obtain

$$\beta_H(t) = t^{-\frac{1}{2}(M-N)} \bar{K}_{\lambda\lambda'}(t) \left(\frac{q_{t13} q_{t24}}{s_0} \right)^{\alpha(t)-M} \bar{\gamma}_H(t) \tag{6.2.29}$$

where the $\bar{\gamma}_H(t)$ are free of kinematical singularities, but may have to satisfy threshold constraints like (6.2.16).

If one pair of masses is equal, say $m_1 = m_3$, then $z_t \sim t^{\frac{1}{2}}$, while if $m_2 = m_4$ also then z_t is finite at $t = 0$, and in both cases the pseudo-thresholds move to $t = 0$. The minimum kinematical behaviour can be deduced by repeating the above argument. It is also necessary to ensure factorization like (6.2.28) for amplitudes which have equal masses in one state but not the other, and we find

$$\begin{aligned} \beta_H(t) &= t^\delta \bar{K}_{\lambda\lambda'}(t) \left(\frac{q_{t13} q_{t24}}{s_0} \right)^{\alpha(t)-M} \bar{\gamma}_H(t) \\ &\equiv K_{\lambda\lambda'}(t) \left(\frac{q_{t13} q_{t24}}{s_0} \right)^{\alpha(t)-M} \bar{\gamma}_H(t) \end{aligned} \tag{6.2.30}$$

where $K_{\lambda\lambda'}(t)$ is given in table 6.1 (for evasion – see section 6.5).

When (6.2.30) is substituted in (4.6.4) and we use the asymptotic form (B.25), (6.2.26), for the rotation function, the Regge pole contribution to a scattering amplitude becomes

$$\begin{aligned} A_{H_t}^R(s, t) &= -16\pi(-1)^A K_{\lambda\lambda'}(t) \bar{\gamma}_H(t) (e^{-i\pi\alpha} + \mathcal{S}) \\ &\times \left\{ \frac{1}{2 \sin \pi(\alpha - v)} \frac{(2\alpha)! (2\alpha + 1)}{[(\alpha + M)! (\alpha - M)! (\alpha + N)! (\alpha - N)!]^{\frac{1}{2}}} \right\} \\ &\times \left(\frac{s-u}{8s_0} \right)^{\alpha(t)-M} \xi_{\lambda\lambda'}(z_t) \end{aligned} \tag{6.2.31}$$

(where A is defined in (B.10)) after some use of the relation

$$(-\alpha)! = \frac{\pi}{\sin \pi\alpha(\alpha - 1)!} \tag{6.2.32}$$

The same result is obtained from (4.6.2) using (B.12) for $\text{Re} \{ \alpha \} > -\frac{1}{2}$.

Table 6.1 Kinematical factors for a *t*-channel helicity amplitude

The factors introduced in (6.2.9) and (6.2.30) are:

$$K_{\lambda\lambda'}(t) \equiv t^\delta \bar{K}_{\lambda\lambda'}(t)$$

$$\bar{K}_{\lambda\lambda'}(t) \equiv (T_{13}^+)^{M-Y_{13}^+} (T_{13}^-)^{M-Y_{13}^-} (T_{24}^+)^{M-Y_{24}^+} (T_{24}^-)^{M-Y_{24}^-}$$

where

$$M \equiv \max\{|\lambda|, |\lambda'|\}, \quad N \equiv \min\{|\lambda|, |\lambda'|\}, \quad \lambda \equiv \lambda_1 - \lambda_3, \quad \lambda' \equiv \lambda_2 - \lambda_4$$

$$T_{ij}^\pm \equiv [t - (m_i \pm m_j)^2]^\pm$$

$$Y_{ij}^\pm \equiv \sigma_i + \sigma_j - \frac{1}{2}[1 - \eta P_i P_j (-1)^{\sigma_i \pm \sigma_j - v}]$$

$$v = 0/\frac{1}{2} \text{ for even/odd fermion number}$$

Evasion

$$\text{UU } \delta = -\frac{1}{2}(M - N)$$

$$\text{EU } \delta = \frac{1}{2}[|\lambda'| - M] + \frac{1}{4}[1 - \eta(-1)^\lambda]$$

$$\text{EE } \delta = \frac{1}{4}[1 - \eta(-1)^\lambda] + \frac{1}{4}[1 - \eta(-1)^{\lambda'}]$$

Conspiracy of Toller number A (see (6.5.10))

$$\text{UU } \delta = \frac{1}{2}\{|A - M| + |A - N|\} - M$$

$$\text{EU } \delta = \frac{1}{2}\{|A - |\lambda'| - M| + \frac{1}{4}\{1 - \eta\bar{\eta}(-1)^\lambda + \epsilon(A - 2\sigma_1)\}\}$$

$$\text{EE } \delta = \frac{1}{2}\{2 + \eta\bar{\eta}(-1)^\lambda + \eta\bar{\eta}(-1)^{\lambda'} + \epsilon(A - 2\sigma_1) + \epsilon(A - 2\sigma_2)\}$$

$$\text{where } \bar{\eta} = (-1)^{A+1} \text{ or } (-1)^{2\sigma+1} \text{ for } 2\sigma \geq A$$

$$\epsilon(A - 2\sigma) = A - 2\sigma \text{ for } A - 2\sigma \geq 0$$

$$= 0 \text{ for } A - 2\sigma \leq 0$$

U \equiv unequal-mass vertex, E \equiv equal-mass vertex. For EU we take $m_1 = m_3$, $m_2 \neq m_4$ so that $\lambda \equiv \lambda_1 - \lambda_3$ is the helicity change at the equal-mass end. In this section we have discussed the evasive case – see section 6.5 for conspiracies.

6.3 Nonsense factors

Equation (6.2.31) is still not satisfactory, however, because the various factorials which appear would introduce singularities at the nonsense values of α (see section 4.5) which cannot be present in the scattering amplitude. So $\bar{\gamma}_H(t)$ must contain suitable factors to cancel them.

Since (Magnus and Oberhettinger 1949, p. 1)

$$(2\alpha)! = \frac{2^{2\alpha+1}(\alpha)!(\alpha + \frac{1}{2})!}{\pi^{\frac{1}{2}}(2\alpha + 1)} \tag{6.3.1}$$

we can re-express the factor in braces { } in (6.2.31) in the form

$$\bar{f}_H(\alpha) \equiv \frac{2^{2\alpha+1}}{\pi^{\frac{1}{2}}} \frac{(\alpha)!(\alpha + \frac{1}{2})!}{[(\alpha + M)!(\alpha - M)!(\alpha + N)!(\alpha - N)!]^{\frac{1}{2}}} \frac{1}{\sin \pi(\alpha - v)} \tag{6.3.2}$$

Now $(\alpha + \frac{1}{2})!$ has simple poles at $\alpha = -\frac{3}{2}, -\frac{5}{2}, \dots$, while $\alpha!$ has poles

at $\alpha = -1, -2, \dots$. But one of these sets of singularities will be cancelled by the denominator, depending on whether M, N are integers of half-integers (i.e. on whether the channel has even or odd fermion number). So we require that $\bar{\gamma}_H(t) \sim [(\alpha + \frac{1}{2} - v)!]^{-1}$ to cancel the others (v is defined in (4.5.6)). In fact such a behaviour of the residue is guaranteed by the Froissart–Gribov projection (4.5.7) because of (B.24).

The remainder has the form

$$\frac{(\alpha + v)!}{[(\alpha + M)! (\alpha - M)! (\alpha + N)! (\alpha - N)!]^{\frac{1}{2}} \sin \pi(\alpha - v)} \tag{6.3.3}$$

which when $\alpha \rightarrow J_0$, where $J_0 - v$ is an integer, has the behaviour

$$\begin{aligned} &(\alpha - J_0)^{-1} \quad \text{for } J_0 \geq M \quad \text{and } v > J_0 > -N \\ &(\alpha - J_0)^{-\frac{1}{2}} \quad \text{for } M > J_0 \geq N \quad \text{and } -N > J_0 \geq -M \\ &\text{Finite for } N > J_0 \geq v \quad \text{and } J_0 < -M \end{aligned}$$

We remember that only the points $J_0 \geq M$ make any physical sense, i.e. are sense–sense (ss) points in the terminology of section 4.5, and so the poles in this region correspond to physical particles. (Note that they are cancelled for alternate J_0 by the signature factor.) At the sense–nonsense (sn) points (6.3.3) behaves like $(\alpha - J_0)^{-\frac{1}{2}} (\alpha + J_0 + 1)^{-\frac{1}{2}}$, but these branch points (which since α is a function of t give branch points in t) cannot be present in the scattering amplitude, so either

$$\bar{\gamma}_H(t) \sim (\alpha - J_0)^{-\frac{1}{2}} (\alpha + J_0 + 1)^{-\frac{1}{2}} \quad \text{or} \quad \bar{\gamma}_H(t) \sim (\alpha - J_0)^{\frac{1}{2}} (\alpha + J_0 + 1)^{\frac{1}{2}}.$$

The Froissart–Gribov projection (4.5.7) gives the former behaviour, but, as discussed in section 4.8, we expect that SCR will hold, in which case the latter behaviour will occur (except perhaps at wrong-signature points where Gribov–Pomeranchuk fixed poles may be expected). Now factorization of the form (6.2.8) requires that

$$\beta_{ss} \beta_{nn} = (\beta_{sn})^2 \propto (\alpha - J_0) (\alpha + J_0 + 1) \tag{6.3.4}$$

where s and n are sense and nonsense values of λ, λ' for the given J_0 . So since the ss residue is expected to be finite to give the physical pole there must be a vanishing of the nn residue. If this behaviour holds at every nonsense point we have

$$\bar{\gamma}_H(t) \sim \left(\frac{(\alpha + M)! (\alpha + N)!}{(\alpha - M)! (\alpha - N)!} \right)^{\frac{1}{2}} \tag{6.3.5}$$

Combining this with the previous requirements we can write

$$\bar{\gamma}_H(t) = \gamma_\lambda(t) \gamma_{\lambda'}(t) \frac{2^{M-1}}{\pi^{\frac{1}{2}}} \frac{1}{(\alpha + \frac{1}{2} - v)!} \left(\frac{(\alpha + M)! (\alpha + N)!}{(\alpha - M)! (\alpha - N)!} \right)^{\frac{1}{2}} \tag{6.3.6}$$

where $\gamma_\lambda(t) \gamma_{\lambda'}(t)$ is a factorized residue free of any special requirements at the nonsense points; and in (6.2.31) this gives

$$A_{H_t}^R(s, t) = -16\pi(-1)^\Lambda K_{\lambda\lambda'}(t) \gamma_\lambda(t) \gamma_{\lambda'}(t) \times (e^{-i\pi(\alpha-v)} + \mathcal{S}) f_H^s(\alpha) \left(\frac{s-u}{2s_0}\right)^{\alpha-M} \xi_{\lambda\lambda'}(z_t) \quad (6.3.7)$$

where
$$f_H^s(\alpha) \equiv \frac{(\alpha+v)!}{(\alpha-M)!(\alpha-N)!} \frac{1}{2\sin\pi(\alpha-v)} \quad (6.3.8)$$

(where $s \equiv$ sense-choosing; see below).

At right-signature points, where the signature factor is finite, (6.3.7) has the behaviour

- (i) $(\alpha - J_0)^{-1}$ for $J_0 \geq M$
- (ii) Finite for $M > J_0 \geq N$ and $J_0 < 0$
- (iii) $(\alpha - J_0)$ for $N > J_0 \geq v$

At wrong-signature points the signature factor behaves like $i(\alpha - J_0)$ giving a finite behaviour for (i), zero for (ii) and double zero for (iii).

However, there are various further considerations which may cause us to modify these conclusions for $\sigma_T \geq J_0$ ($\sigma_T \equiv \max\{\sigma_1 + \sigma_3, \sigma_2 + \sigma_4\}$).

a. Ghost-killing factors

If the trajectory passes through a right-signature point for $t < 0$ the ss residue must vanish, otherwise there would be a ‘ghost’ particle of negative m^2 , i.e. a ‘tachyon’. Since the Froissart bound restricts trajectories to $\alpha < 1$ for $t < 0$ this difficulty only occurs for even-signature trajectories at $J - v = 0$, which we see from figs. 5.4–5.6 applies in practice only to the f, A_2 and $K^{**}(1400)$ trajectories (and perhaps the P – see section 6.8b) at $\alpha = 0$. If such a zero is inserted in the ss residue it must also appear in the sn and nn residues because of (6.3.4). This is sometimes called the ‘Chew mechanism’ (Chew 1966).

b. Choosing nonsense

At a given nonsense J_0 a trajectory may ‘choose’ to satisfy (6.3.4) by having β_{nn} finite and $\beta_{ss} = 0$ instead. This gives

$$\bar{\gamma}_H(t) \sim [(\alpha - J_0)(\alpha + J_0 + 1)]^{\frac{1}{2}}$$

for $M > J_0 \geq N$ as before, but $\bar{\gamma}_H(t) \approx (\alpha - J_0)(\alpha + J_0 + 1)$ for some sense points $J_0 \geq M$. If this happens say for $p > J_0 > M$, where $p - v$ is some integer $> M$, then we have

$$\bar{\gamma}_H(t) \sim \frac{(\alpha + p)!}{(\alpha - p)!} \left(\frac{(\alpha - M)! (\alpha - N)!}{(\alpha + M)! (\alpha + N)!} \right)^{\frac{1}{2}} \tag{6.3.9}$$

instead of (6.3.5). The resulting pole in the nn amplitudes cannot correspond to a physical particle of course, and so it must be cancelled (or compensated for). Since the asymptotic behaviour of $e_{\lambda\lambda}^{-\alpha-1}(z_t)$ at a nn point is $z^{-\alpha-1}$, not z^α , the compensating trajectory must pass through $-J_0 - 1$. This is sometimes called the ‘Gell–Mann mechanism’ (Gell–Mann and Goldberger 1962, Gell–Mann *et al.* 1964).

However, the need for such a compensating trajectory can be avoided by putting a zero in the nn residue, in which case extra zeros will also appear in the sn and ss residues through (6.3.4). This is called the ‘no compensation mechanism’.

c. Wrong-signature fixed poles

The arguments of section 4.8 have led us to expect fixed poles (or infinite square-root branch points) at wrong-signature nonsense points. They will not contribute to the asymptotic behaviour of the scattering amplitude because of the signature factor. However, if they are present in the residue of a Regge pole they will cancel the zero from the signature factor.

The fixed poles, which stem from the presence of the third double spectral function ρ_{su} , could be additional to the Regge poles, and not present in the Regge residues. Or, even if fixed poles are present in the residue, since at the point where $\alpha = J_0$ (J_0 being a wrong-signature nonsense point) the residue obtains a contribution only from ρ_{su} , while at all other values of α it receives contributions from all three double spectral functions, the residue might well behave like

$$a(t) + b(t) (\alpha(t) - J_0)$$

for example. So with $b \geq a$ there would still be a zero near $\alpha(t) = J_0$, but with $a \geq b$ there would not.

Table 6.2 summarizes the above possibilities for the behaviour of the residue, and the corresponding behaviour of the Regge pole amplitude.

The chief importance of these results is that in some cases the Regge

Table 6.2 *The behaviour of the residue and amplitude as a trajectory passes through a nonsense point, J_0*

	Residue			Mechanism	Amplitude		
	nn	sn	ss		nn	sn	ss
Right-signature	$\alpha - J_0$	$(\alpha - J_0)^{\frac{1}{2}}$	1	Sense-choosing	$\alpha - J_0$	1	$(\alpha - J_0)^{-1}$
	1	$(\alpha - J_0)^{\frac{1}{2}}$	$\alpha - J_0$	Nonsense-choosing	1	1	1
	$(\alpha - J_0)^2$	$(\alpha - J_0)^{\frac{3}{2}}$	$\alpha - J_0$	Chew mechanism	$(\alpha - J_0)^2$	$\alpha - J_0$	1
	$\alpha - J_0$	$(\alpha - J_0)^{\frac{3}{2}}$	$(\alpha - J_0)^2$	No compensation	$\alpha - J_0$	$\alpha - J_0$	$\alpha - J_0$
Wrong-signature	$(\alpha - J_0)^{-1}$	$(\alpha - J_0)^{-\frac{1}{2}}$	1	Fixed pole	1	1	1

In the above we have assumed the presence of a fixed pole in the residue at the wrong-signature point. If this is absent the residue behaves in the same way as at the corresponding right-signature point, and the amplitude is the same except for an extra $\alpha - J_0$ from the signature factor.

pole amplitude is predicted to have a zero in t . A good example of this is the process $\pi^+p \rightarrow \pi^0n$ which in the t channel ($\pi^+\pi^0 \rightarrow \bar{p}n$) contains only the ρ trajectory from our list in table 6.5. From fig. 5.5 (and see also fig. 6.6a below) this trajectory is approximately $\alpha(t) = 0.5 + 0.9t$, and so $\alpha(t) = 0$ for $t \approx -0.55 \text{ GeV}^2$. The t -channel helicity amplitudes for this process are A_{++} and A_{+-} (defined in (4.3.11)) and $\alpha = 0$ is a ss point for A_{++} ($\lambda = \lambda' = 0$) but a sn point for A_{+-} ($\lambda = 0, \lambda' = 1$), and is a wrong-signature point for the ρ trajectory since the ρ resonance has spin = 1. So from table 6.2 we see that if there is no fixed pole and the trajectory chooses sense then A_{++} will be finite but A_{+-} will vanish at $t = -0.55$, while both amplitudes will vanish if it chooses nonsense, or both will be finite if there is a strong fixed-pole contribution. (The nonsense-nonsense amplitude occurs in $\bar{p}n \rightarrow \bar{p}n$ and does not have to be considered here.) The data on this process (fig. 6.1) show a dip but not a zero of $d\sigma/dt$ at this point, suggesting that the ρ chooses sense. But the conclusion depends on what other singularities may be present, such as a lower lying ρ' trajectory, Regge cuts etc. We shall return to this problem in section 6.8k, and an alternative explanation of the structure involving cuts will be presented in section 8.7c.

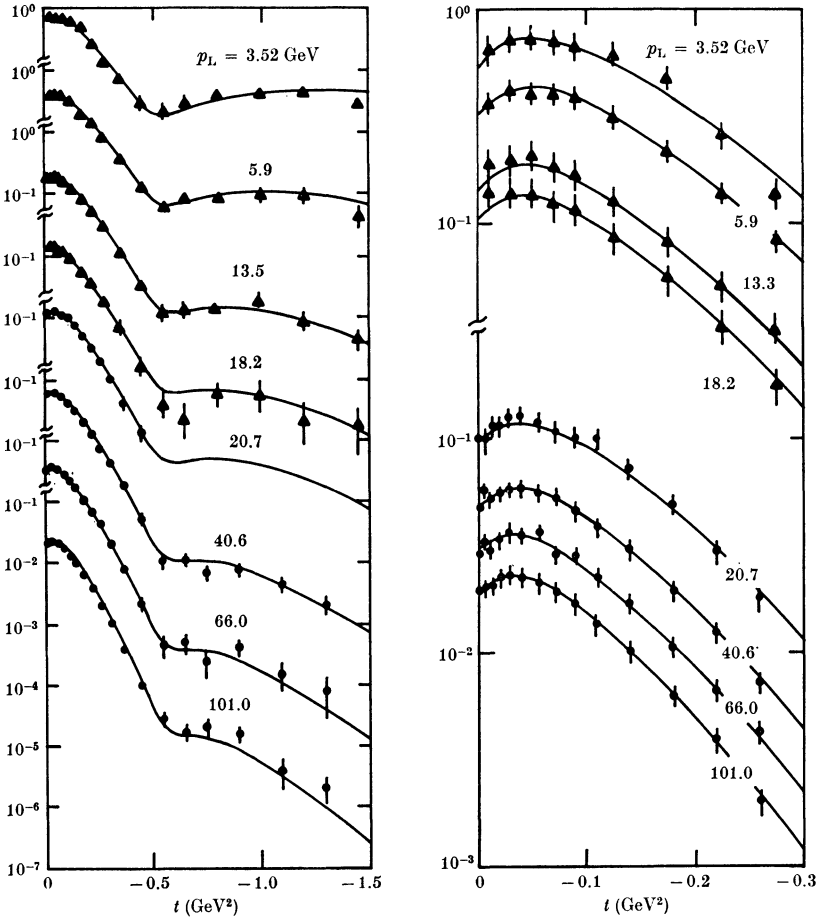


FIG. 6.1 Data for $d\sigma/dt(\pi^-p \rightarrow \pi^0n)$ at various laboratory momenta p_L . The lines are a fit with ρ and ρ' trajectories, from Barger and Phillips (1974).

6.4 Regge poles and s-channel amplitudes

In section 6.2 we went to a good deal of trouble to ensure that we incorporated the correct kinematical t factors into the Regge residues in the t -channel helicity amplitudes. However, many of these factors cancel out when we construct measurable quantities such as $d\sigma/dt$, density matrices etc., and the only essential t -singularities are those in the s -channel half-angle factors $\xi_{\mu\mu'}(z_s)$. It is obvious therefore that there would be many advantages to working directly with t -channel Regge poles in s -channel helicity amplitudes. But if we wish to do this

we have to be rather careful about the extra t factors which were introduced because the Reggeon has a definite parity in the t channel, and because its residue must factorize in terms of t -channel helicities, and we must include the various nonsense factors discussed in the previous section.

The expression (Cohen-Tannoudji, Morel and Navelet 1968, Le Bellac 1968)

$$A_{H_s}^R(s, t) = - \left(\frac{s}{s_0} \frac{1-z_s}{2} \right)^{\frac{1}{2}|\mu-\mu'|} \left(\frac{1+z_s}{2} \right)^{\frac{1}{2}|\mu+\mu'|} \times \left(\frac{e^{-i\pi(\alpha-v)} + \mathcal{P}}{2 \sin \pi(\alpha-v)} \right) \beta_{H_s}(t) \left(\frac{s-u}{2s_0} \right)^{\alpha(t)} \tag{6.4.1}$$

contains the half-angle factor and signature factor. And since, from (1.7.17),

$$\left(\frac{s}{s_0} \frac{1-z_s}{2} \right)^{\frac{1}{2}|\mu-\mu'|} \xrightarrow{s \rightarrow \infty} \left(\frac{-t}{s_0} \right)^{\frac{1}{2}(\mu-\mu')} = \left(\frac{-t}{s_0} \right)^{\frac{1}{2}n} \tag{6.4.2}$$

is independent of s (where

$$n \equiv ||\mu_1 - \mu_2| - |\mu_3 - \mu_4|| \tag{6.4.3}$$

is the net helicity-flip in the s channel) (6.4.1) has the Regge behaviour $\sim (s/s_0)^{\alpha(t)}$. But it does not satisfy t -channel factorization.

For unequal masses we have found that the Regge residue must behave like $t^{\frac{1}{2}(M-N)-\alpha}$ for $t \rightarrow 0$, and so the t -channel helicity amplitudes (6.2.31) have the behaviour

$$A_{H_t}^R(s, t) \sim (-t)^{\frac{1}{2}(M+N)} = (-t)^{\frac{1}{2}(|\lambda_1-\lambda_3|+|\lambda_2-\lambda_4|)} \tag{6.4.4}$$

Now as $t \rightarrow 0$ crossing angles (4.3.5) all have the behaviour

$$\chi_i \sim \sin \chi_i \sim (-t)^{\frac{1}{2}}, \quad \text{and so } d_{\lambda_i \mu_i}^{\sigma_i}(\chi_i) \sim (-t)^{\frac{1}{2}|\lambda_i - \mu_i|}$$

for $i = 1, \dots, 4$. Hence the helicity crossing matrix (4.3.7)

$$M(H_s, H_t) \sim (-t)^{\frac{1}{2}(|\lambda_1-\mu_1|+|\lambda_2-\mu_2|+|\lambda_3-\mu_3|+|\lambda_4-\mu_4|)} \tag{6.4.5}$$

is diagonal to first order in t at $t = 0$. Substituting (6.4.4) and (6.4.5) in (6.3.7) we deduce

$$A_{H_s}^R(s, t) \sim \sum_{H_t} (-t)^{\frac{1}{2}(|\lambda_1-\mu_1|+|\lambda_2-\mu_2|+|\lambda_3-\mu_3|+|\lambda_4-\mu_4|+|\lambda_1-\lambda_3|+|\lambda_2-\lambda_4|)} \tag{6.4.6}$$

and the minimal kinematical behaviour is obtained from those terms in the sum over the λ_i where $\lambda_i = \mu_i, i = 1, \dots, 4$, and so

$$A_{H_s}^R(s, t) \sim (-t)^{\frac{1}{2}(|\mu_1-\mu_3|+|\mu_2-\mu_4|)}, \quad t \rightarrow 0 \tag{6.4.7}$$

To ensure this behaviour we write instead of (6.4.1)

$$A_{H_s}^R(s, t) = - \left(\frac{-t}{s_0} \right)^{\frac{1}{2}(|\mu_1 - \mu_3| + |\mu_2 - \mu_4| - |\mu' - \mu|)} \left(\frac{s}{s_0} \frac{1 - z_s}{2} \right)^{\frac{1}{2}|\mu' - \mu|} \times \left(\frac{1 + z_s}{2} \right)^{\frac{1}{2}|\mu + \mu'|} \frac{e^{-i\pi(\alpha - v)} + \mathcal{S}}{2 \sin \pi(\alpha - v)} \gamma_{H_s}(t) \left(\frac{s - u}{2s_0} \right)^{\alpha(t)} \tag{6.4.8}$$

$$\xrightarrow{s \rightarrow \infty} - \left(\frac{-t}{s_0} \right)^{\frac{1}{2}m} \frac{e^{-i\pi(\alpha - v)} + \mathcal{S}}{2 \sin \pi(\alpha - v)} \gamma_{H_s}(t) \left(\frac{s}{s_0} \right)^{\alpha(t)} \tag{6.4.9}$$

where $m \equiv |\mu_1 - \mu_3| + |\mu_2 - \mu_4|$ (6.4.10)

and $\gamma_{H_s}(t)$ is factorizable in terms of s -channel helicities

$$\gamma_{H_s}(t) = \gamma_{\mu_1 \mu_3}(t) \gamma_{\mu_2 \mu_4}(t) \tag{6.4.11}$$

and is free of kinematical singularities.

Though this deduction has been made for unequal masses, it is in fact valid for any mass combination because $A_{H_s}(s, t)$ has no t -singularities which depend on the masses except for those in the half-angle factor.

The only difficulty with this method is that one cannot easily incorporate the nonsense mechanisms. There is no problem with the nonsense-choosing, no-compensation or fixed-pole mechanisms which give the same behaviour for all the t -channel amplitudes (see table 6.2), and hence for all the s -channel amplitudes. But the sense-choosing and Chew mechanisms give zeros in some t -channel amplitudes but not others, and if a given A_{H_t} vanishes there will be constraints like $\sum_{H_t} M(H_s, H_t)^{-1} A_{H_s}(s, t) \sim \alpha(t) - J_0$ (6.4.12)

(where M^{-1} is the inverse matrix of M) which are difficult to parameterize. But apart from these cases (6.4.8) has much to recommend it.

6.5 Daughters and conspirators*

In obtaining (6.3.7) for the contribution of a Regge pole to a scattering amplitude we made use of (6.2.26) for the asymptotic behaviour of the rotation function. However, it is evident from (1.7.15), (1.7.19) that for unequal masses, for $t \rightarrow 0$, $q_t \sim t^{-\frac{1}{2}}$ and $z_t \rightarrow \epsilon$ ($= \pm 1$, see (6.2.19)) for all s . This might seem to imply that the unequal-mass scattering amplitude will not have Regge asymptotic behaviour at $t = 0$. But in fact this cannot be true, because $t = 0$ is not a singular point of the reduced scattering amplitude \hat{A}_{H_t} .

* This section may be omitted at first reading.

It is easier to see what has gone wrong if we rewrite (1.7.19) as

$$z_t = \frac{s}{2q_{t13}q_{t24}} \left(1 + \frac{\Delta(t)}{s} \right) \tag{6.5.1}$$

where
$$\Delta(t) \equiv \frac{1}{2t} [t^2 - t\Sigma + (m_1^2 - m_3^2)(m_2^2 - m_4^2)] \tag{6.5.2}$$

is singular at $t = 0$ for unequal masses, and then make the expansion

$$e_{\lambda\lambda}^{-g-1}(z_t) = \xi_{\lambda\lambda}(z_t) f(\alpha) \left[\left(\frac{z_t}{2} \right)^{\alpha-M} + f_1(\alpha) \left(\frac{z_t}{2} \right)^{\alpha-M-2} + \dots \right]$$

where $f(\alpha)$ is given by (B.25) and $f_1(\alpha)$ can be deduced from (B.24). Substituted in (4.6.4) with (6.5.1) and (6.2.30), this gives

$$A_{Ht}^R(s, t) \propto \left\{ \left(\frac{s}{4s_0} \right)^{\alpha-M} + \Delta(t) (\alpha - M) 4s_0 \left(\frac{s}{4s_0} \right)^{\alpha-M-1} + \left[\frac{(\alpha - M)(\alpha - M - 1)}{2} (4s_0 \Delta(t))^2 + a_1(\alpha) \left(\frac{q_{t13}q_{t24}}{s_0} \right)^2 \right] \left(\frac{s}{4s_0} \right)^{\alpha-M-2} + \dots \right\} \tag{6.5.3}$$

So each term in the expansion of order $(s/4s_0)^{\alpha-M-n}$ has a t^{-n} singularity at $t = 0$. It is these singularities which cause the problem.

However, the amplitude must be analytic at $t = 0$, since it is supposed to obey the Mandelstam representation, so there must be some other contributions which cancel them. These could be contained in the background integral (see Collins and Squires (1968), chapter 3), but a more popular suggestion (Freedman and Wang 1967) is that there are further trajectories known as ‘daughters’ which have singular residues which precisely cancel the singularities of the original ‘parent’ trajectory. So the first daughter will have

$$\alpha_1(t) \xrightarrow{t \rightarrow 0} \alpha(t) - 1 \tag{6.5.4}$$

and residue

$$\beta_1(t) \xrightarrow{t \rightarrow 0} -\beta(0) \frac{(m_1^2 - m_3^2)(m_2^2 - m_4^2)(\alpha(0) - M) 2s_0}{t} + \text{non-singular terms} \tag{6.5.5}$$

to cancel the second term in (6.5.3). In fact an infinite sequence of daughters is needed with

$$\alpha_k(0) = \alpha(0) - k, \quad k = 1, 2, 3, \dots, \quad \beta_k(0) \underset{t \rightarrow 0}{\sim} t^{-k} \tag{6.5.6}$$

The odd-numbered daughters must have opposite signature to the parent, i.e. $\mathcal{S}_k = \mathcal{S}(-1)^k$, so that their signature factors are identical to those of the parent at $t = 0$.

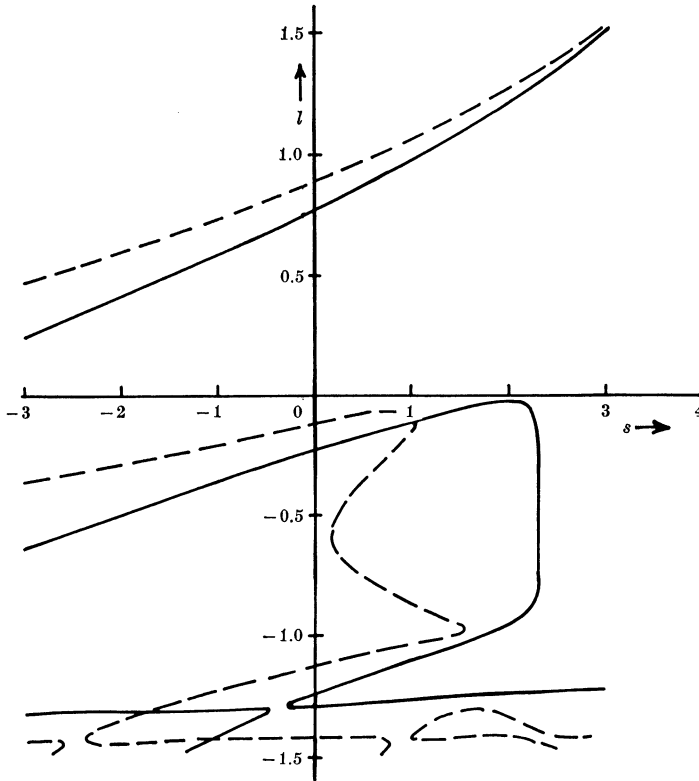


FIG. 6.2 Regge trajectories obtained by Cutkosky and Deo (1967) from the Bethe–Salpeter equation using a potential with a repulsive core. The continuous and dashed curves represent different coupling strengths. The strange behaviour of the daughters is evident.

There is not a great deal of evidence for the existence of such daughters in figs. 5.4–5.6. Indeed, calculations of trajectories using unequal-mass kinematics in the Bethe–Salpeter equation (Cutkosky and Deo 1967) produce a rather peculiar behaviour for the daughters (fig. 6.2) which do not manifest themselves as particles. Unless the non-singular terms in (6.5.5) are important, the daughters need not be visible in the s -channel energy dependence either, since their main purpose is to ensure the $s^{\alpha(t)}$ behaviour for all t , and they may be masked by other singularities (cuts etc.). But we shall discuss in the next chapter further reasons why such trajectories should exist parallel to the parent (see fig. 7.5 below).

Another problem for Regge poles at $t = 0$ is that the residues cannot have the kinematically expected behaviour (6.2.23) but only (6.2.25)

(neglecting factorization for the moment). This is because, as can be deduced from (6.2.22), the definite-parity amplitudes must satisfy the constraint

$$\hat{A}_{H_i}^\eta(s, t) \mp \eta \hat{A}_{H_i}^{-\eta}(s, t) \underset{t \rightarrow 0}{\sim} t^N \tag{6.5.7}$$

In using (6.2.25) we make the Regge pole ‘evade’ this constraint by including an extra factor t^N in its residue. This is necessary because a Reggeon can occur in only one parity amplitude.

However, if there were two trajectories of opposite parity they could ‘conspire’ together to satisfy (6.5.7) (Leader 1968, Capella, Tran Thanh Van and Contogouris 1969, Wang and Wang 1970). This would require

$$\alpha_+(0) = \alpha_-(0) \quad \text{and} \quad \beta_H^\pm(t) \pm \beta_{\bar{H}}(t) \underset{t \rightarrow 0}{\sim} t^{\frac{1}{2}(M+N)-\alpha} \tag{6.5.8}$$

where \pm refers to the parity $\eta = \pm 1$. Such a conspiracy would give

$$\beta_H^\eta(t) \underset{t \rightarrow \infty}{\sim} t^{\frac{1}{2}(M-N)-\alpha}, \quad \eta = \pm 1 \tag{6.5.9}$$

instead of (6.2.29) which behaves like $\sim t^{\frac{1}{2}(M+N)-\alpha}$.

This behaviour clearly does not factorize between λ and λ' , but we are none the less free to choose that a particular amplitude with $\lambda = \lambda' = A$ say, where A is a given number called the ‘Toller number’, has this most singular permissible behaviour. Factorization then demands that the other helicity amplitudes have

$$\beta_{\lambda\lambda'}^\eta(t) \sim t^{\frac{1}{2}(|A-\lambda|+|A-\lambda'|)-\alpha} \tag{6.5.10}$$

and for a conspiring trajectory the parameter δ is replaced by the values in table 6.1 (p. 160). Applying the crossing relation (4.3.7) with (6.4.5) we find

$$A_{H_s}^R(s, t) \sim (-t)^{\frac{1}{2}(|A-\mu_1-\mu_3|+|A-\mu_2-\mu_4|)} \tag{6.5.11}$$

so unlike (6.4.7) an amplitude with $|\mu_1 - \mu_3| = |\mu_2 - \mu_4| = A$ will not vanish at $t = 0$.

A simple example is provided by the process $\gamma p \rightarrow \pi^+ n$ which should be dominated by π -exchange near the forward direction ($t \approx 0$). Since for the photon $\mu_1 = \pm 1$ only, and the spinless pion has $\mu_3 = 0$ only, we see from (6.4.10) that $m \neq 0$ and so with the behaviour (6.4.7) all the amplitudes will vanish at $t = 0$, and hence a dip must occur in $d\sigma/dt$ at $t = 0$. In fact the data show a sharp forward spike of width $\Delta t \approx m_\pi^2$ which could be explained by a $A = 1$ conspiracy between the π and a similar natural-parity trajectory giving the behaviour (6.5.11) instead (Ball, Frazer and Jacob 1968). However, a scalar particle similar to the pion does not occur, and it has been shown (Le Bellac 1967) that such a conspiracy is incompatible with factorization in other π -exchange process, so it now seems more likely that the presence

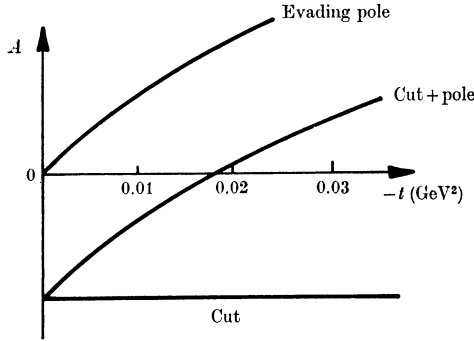


FIG. 6.3 The scattering amplitude for $\gamma p \rightarrow \pi^+ n$ showing the contributions of an evasive pion pole and a Regge cut. Cut + pole gives the sharp forward peak seen in the data.

of Regge cuts accounts for the forward peak (see fig. 6.3 and section 8.7*f*). There does not seem to be any evidence for conspiracies of meson trajectories.

A conspiracy is essential, however, if the fermion number of the exchange is odd. We mentioned after (6.2.25) that in this situation multiplying the residue by t^N would introduce a spurious square-root branch point at $t = 0$. In fact making the replacement $\sqrt{t} \rightarrow -\sqrt{t}$ in (6.2.24) we find that for half-integer λ, λ'

$$A_{H_t}^{\eta}(s, \sqrt{t}) = A_{\bar{H}_t}^{\eta}(s, -\sqrt{t}) (-1)^{|\lambda - \epsilon\lambda'|} \tag{6.5.12}$$

This is called the generalized MacDowell symmetry (after MacDowell 1959), and it means that for baryons there must be a conspiracy between opposite parity trajectories of Toller number $A = \frac{1}{2}$, so

$$\alpha^+(\sqrt{t}) = \alpha^-(-\sqrt{t}) \quad \text{and} \quad \beta_H^+(\sqrt{t}) = (-1)^{|\lambda - \epsilon\lambda'|} \beta_{\bar{H}}(-\sqrt{t}) \tag{6.5.13}$$

If such trajectories are even in \sqrt{t} , like the linear form (5.3.2), then the two trajectories should coincide, and one would expect baryons to occur in degenerate doublets of opposite parity. The inclusion of terms which are odd in \sqrt{t} , such as

$$\alpha^{\pm}(\sqrt{t}) = \alpha_0 \pm \alpha_1\sqrt{t} + \alpha_2 t + \dots \tag{6.5.14}$$

splits the degeneracy, but makes the trajectories curved. However, we found in section 5.3 that baryon trajectories appear to be linear in t , but not parity doubled. It is possible to put zeros into the residues to make the unwanted states vanish (see for example Storror (1972, 1975)), or to introduce a branch point at $J = \alpha_0$, and place the unwanted states on the unphysical side of the cut (see for example Carlitz and

Kisslinger (1970) and section 8.7*i*), but the correct explanation for this problem is still unclear.

6.6 Group theoretical methods*

These daughter and conspiracy problems arise from the fact that the rotation functions $d_{\lambda\lambda'}^J(z_t)$ are not an appropriate way of representing the scattering amplitude at $t = 0$ because of (6.5.2). The work of Toller (1965, 1967) and others has given a somewhat more general view of these difficulties.

In writing the partial-wave series (4.4.14) we decomposed the scattering amplitude in terms of representation functions of the three-dimensional rotation group $O(3)$, or more strictly, since half-integer spins may be included, its covering group $SU(2)$. The rotation group is the so-called 'little group' of the inhomogeneous Lorentz group, or Poincaré group \mathcal{P} , i.e. it is the group of transformations which leaves invariant the total four-momentum of the incoming or outgoing particles (in the t channel)

$$P_\mu \equiv (p_{1\mu} + p_{3\mu}) = (p_{2\mu} + p_{4\mu}), \quad \mu = 1, \dots, 4 \quad (6.6.1)$$

(see for example Martin and Spearman (1970) chapter 3, and Britten and Barut (1964)). The angular momentum J^2 is of course a Casimir operator of this little group, and $\sum_\mu P_\mu^2 \equiv t$ is also a Casimir invariant of \mathcal{P} .

However, Wigner (1939) showed that although $O(3)$ is the little group for $t > 0$, there are in fact four different classes of representations of \mathcal{P} characterized by different values of t . These are

- (i) Timelike, $t > 0$, little group $O(3)$
- (ii) Spacelike, $t < 0$, little group $O(2, 1)$
- (iii) Lightlike, $t = 0$, $P_\mu \neq 0$, little group $E(2)$
- (iv) Null, $t = 0$, $P_\mu = 0$, little group $O(3, 1)$

Here $O(3)$ is the rotation group in a space with three real dimensions, with $x^2 + y^2 + z^2 = R^2$ invariant; $O(2, 1)$ is the rotation group in a space with two real dimensions and one imaginary, with $x^2 + y^2 - z^2$ invariant; $E(2)$ is the group of Euclidian transformations in two dimensions; while $O(3, 1)$ is the rotation group in a space with three real dimensions and one imaginary, with $x^2 + y^2 + z^2 - t^2$ invariant, which is isomorphic to the Lorentz group itself.

The representation functions of $O(3)$ are the $d_{\lambda\lambda'}^J(z_t)$, $-1 \leq z_t \leq 1$.

* This section may be omitted on first reading.

The representations of $O(2, 1)$ are again $d_{\lambda\lambda'}^J(z_t)$, but with z_t taking the unphysical values appropriate to $t < 0$. Bargmann (1947) has shown that a function which is square-integrable on this group manifold can be expanded in terms of the principle and discrete series of representations, so that a scattering amplitude expanded in this basis takes the form (Joos 1964, Boyce 1967)

$$A_{H_i}(s, t) = -\frac{16\pi}{2i} \int_{-\frac{1}{2}-i\infty}^{-\frac{1}{2}+i\infty} dJ \frac{2J+1}{\sin \pi(J+\lambda')} A_{HJ}(t) d_{\lambda\lambda'}^J(z_t) + \text{nonsense terms} \quad (6.6.2)$$

i.e. (4.6.2) without any Regge poles or cuts in $\text{Re}\{J\} > -\frac{1}{2}$. This is because the square-integrability condition requires $A_{H_i}(s, t) = O(s^{-\frac{1}{2}})$.

So the Sommerfeld–Watson representation can be regarded as a representation on an $O(2, 1)$ basis. However, the equivalence is incomplete in that the Sommerfeld–Watson representation is valid for all t , not just $t < 0$. Also it is valid for non-relativistic potential scattering which has $E(2)$ rather than $O(2, 1)$ as its little group for $t < 0$, and the $E(2)$ representations are quite different (Inonu and Wigner 1952, Levy-Leblond 1966). And of course with Regge singularities in $\text{Re}\{J\} > -\frac{1}{2}$ the Sommerfeld–Watson representation is an analytic continuation in J of (6.6.2). But if these differences are kept in mind it is possible to rephrase Regge theory as an $O(2, 1)$ decomposition.

Because of the mass-shell conditions $p_1^2 = m_1^2$ etc.,

$$t = (p_1 + p_3)^2 = (p_2 + p_4)^2 = 0$$

implies that the individual components of P_μ are zero in (6.6.1) only if $m_1 = m_3$ and $m_2 = m_4$, so the little group at $t = 0$ will be $O(3, 1)$ or $E(2)$ depending on whether or not the masses are equal.

If the masses are equal then the amplitude can be decomposed in terms of representation functions of $O(3, 1)$ which may be denoted by $d_{T\sigma}^{\Lambda} z_t$. They have been derived by Sciarrino and Toller (1967) and depend upon two Casimir operators, of which one is the Toller number, Λ , introduced in (6.5.10), which can take on the values $0, 1, 2, \dots$ or $\frac{1}{2}, \frac{3}{2}, \frac{5}{2}, \dots$ depending on the fermion number, and the other, σ , is pure imaginary, $-\infty < i\sigma < \infty$. This extra Casimir operator appears because there are two degrees of freedom in satisfying $\sum_{\mu} P_{\mu}^2 = 0$ with equal masses. The other degree of freedom corresponds to variation

of s . On this basis the amplitude can be expanded

$$A_{H_i}(s, t = 0) = \delta_{\lambda\lambda'} \sum_{T, T'} \sum_{\Lambda = -T_M}^{T_M} \int_{-i\infty}^{i\infty} d\sigma (\Lambda^2 - \sigma^2) A_{T\lambda T'}^{A\sigma}(t = 0) d_{T\lambda T'}^{A\sigma}(z_t) \tag{6.6.3}$$

where $A_{T\lambda T'}^{A\sigma}(t)$ are $O(3, 1)$ partial-wave amplitudes, $T_M \equiv \min\{T, T'\}$ and in the summations

$$|\sigma_1 - \sigma_3| \leq T' \leq \sigma_1 + \sigma_3, \quad |\sigma_2 - \sigma_4| \leq T' \leq \sigma_2 + \sigma_4.$$

At $t = 0$ only the non-flip $\lambda = \lambda'$ amplitudes survive.

If we suppose that there is a Toller pole at $\sigma = a$ say (just as there may be a Regge pole at $J = \alpha$ in (6.6.2)) then analytic continuation in σ gives

$$A_{H_i}(s, 0) = [(6.6.3)] + \delta_{\lambda\lambda'} \sum_{T, T'} A_{T\lambda T'}^{Aa} (\Lambda^2 - a^2) d_{T\lambda T'}^{Aa} \tag{6.6.4}$$

where [(6.6.3)] represents the right-hand side of (6.6.3) and Λ is the Toller number of the pole. Since it is found that

$$d_{T\lambda T'}^{A\sigma}(z_t) \underset{z_t \rightarrow \infty}{\sim} (z_t)^{\sigma-1-|\Lambda-\lambda|} \tag{6.6.5}$$

we deduce from (6.6.4) that

$$A_{H_i}(s, 0) \sim \delta_{\lambda\lambda'} (z_t)^{a-1-|\Lambda-\lambda|} \tag{6.6.6}$$

If this is compared with (6.3.7) (remembering (6.5.11)) it will be seen that this behaviour corresponds to a Regge pole with $\alpha(0) = a - 1$ and Toller number Λ . Indeed if these $O(3, 1)$ representation functions are decomposed in terms of $d_{\lambda\lambda'}^J(z_t)$ it is found (Sciarrino and Toller 1967) that the single Toller pole in the σ plane at $\sigma = a$ (6.6.4), corresponds to an infinite sequence of Regge poles in the J plane at $J = \alpha_k(0)$ with $\alpha_k(0) = a - k - 1, \quad k = 0, 1, 2, \dots$ (6.6.7)

i.e. a conspiring daughter sequence of Toller number Λ . As we move away from $t = 0$ the $O(3, 1)$ symmetry is broken so the daughter trajectories do not have to remain integrally spaced from the parent as in (6.6.7).

This argument clearly does not work for unequal masses because the $E(2)$ representations are quite different from those of $O(3, 1)$, so continuation in the masses is needed to justify the use of Toller poles in this case (Domokos and Tindle 1968, Bitar and Tindle 1968, Kuo and Suranyi 1970). Indeed the apparent absence of conspiracies noted in the previous section leads one to suspect that nature has not in fact made use of the extra degree of freedom at $t = 0$ represented by variation of σ in (6.6.3). A single Regge pole at $t = 0$ corresponds to a counter-conspiracy consisting of an infinite sequence of Toller poles

in the σ plane (just like the many-to-one relation between poles in the l and n planes in section 2.10) so the lack of conspiracies presumably reflects the primacy of the J plane over the σ plane. If so, these group-theory techniques do not appear to possess any significant advantage over the conventional Sommerfeld–Watson method which we use in this book.

6.7 Internal symmetry and crossing

a. Isospin

As we mentioned in section 5.2, the approximate invariance of strong interactions under the internal symmetries $SU(2)$ and $SU(3)$ leads to important relations between scattering amplitudes. We begin with the isospin group $SU(2)$ which appears to be broken by at most a few per cent, which is often well within the errors to which scattering amplitudes can be determined. Hence it is frequently more useful to refer to scattering amplitudes for the various possible isospin states, rather than to the amplitudes for the different charge states of the particles involved.

It is convenient to consider first a particle decay such as $a \rightarrow 1 + 2$. The final state may be expressed in terms of the isospins of the particles (see (5.2.1)) as

$$|1, 2\rangle = |I_1, I_{1z}\rangle \oplus |I_2, I_{2z}\rangle \tag{6.7.1}$$

The total isospin is the sum of the isospin vectors of the particles

$$I = I_1 + I_2 \tag{6.7.2}$$

and its possible eigenvalues are

$$I = I_1 + I_2, \quad I_1 + I_2 - 1, \dots, |I_1 - I_2| \tag{6.7.3}$$

while

$$I_z = I_{1z} + I_{2z} = I, \quad I - 1, \dots, -I \tag{6.7.4}$$

so the state (6.7.1) can be written as a superposition of the various possible total isospin states as

$$|1, 2\rangle = \sum_I \langle I_1, I_2, I_{1z}, I_{2z} | I, I_z \rangle |I, I_z\rangle \tag{6.7.5}$$

where $\langle I_1, I_2, I_{1z}, I_{2z} | I, I_z \rangle$ are the Clebsch–Gordan coefficients (see for example Edmonds (1960) chapter 3). Since the particle a has a definite isospin, I_a , only one term in the sum (6.7.5) occurs in the decay process, and so the decay amplitude can be expressed in the form

$$A(a \rightarrow 1 + 2) = \langle I_1, I_2, I_{1z}, I_{2z} | I_a, I_{az} \rangle \bar{A}(a \rightarrow 1 + 2) \tag{6.7.6}$$

where \bar{A} is a ‘reduced’ amplitude which is independent of I_{az} . Thus isospin invariance implies that the different charge states of particle a , with their different values of I_{az} (see (5.2.1)), will have decay rates which are related to each other by the Clebsch–Gordan coefficients of SU(2).

For example in the decay $\rho \rightarrow \pi\pi$ both ρ and π have $I = 1$, and $I_z = 1, 0, -1$ for the charge states $+, 0$ and $-$. So the various decay amplitudes are related according to (6.7.6) by

$$A(\rho^+ \rightarrow \pi^+\pi^0) = A(\rho^- \rightarrow \pi^0\pi^-) = A(\rho^0 \rightarrow \pi^+\pi^-) = \frac{1}{\sqrt{2}}\bar{A}(\rho \rightarrow \pi\pi) \tag{6.7.7}$$

where $\bar{A}(\rho \rightarrow \pi\pi)$ is the reduced amplitude. Such relations appear to be well satisfied in hadronic decays.

Similarly for the scattering process $1 + 2 \rightarrow 3 + 4$, both the initial and final states can be expressed as isospin states, like (6.7.5), and if the process is isospin invariant the scattering amplitude may be decomposed as

$$\langle 34 | A | 12 \rangle = \sum_I \langle I_3, I_4, I_{3z}, I_{4z} | I, I_z \rangle^* \langle I_1, I_2, I_{1z}, I_{2z} | I, I_z \rangle A(I) \tag{6.7.8}$$

where $A(I)$ is independent of I_z . In general the number of different isospin amplitudes is smaller than the number of charged particle processes which can occur and so (6.7.8) inter-relates the amplitudes for the different processes.

For example in πN scattering the state $|\pi^+p\rangle$ has $I_z = 1 + \frac{1}{2} = \frac{3}{2}$ and so $I = \frac{3}{2}$ only. Likewise $|\pi^-n\rangle$ has $I_z = -\frac{3}{2}$, $I = \frac{3}{2}$. Hence from (6.7.8)

$$\langle \pi^+p | A | \pi^+p \rangle = \langle \pi^-n | A | \pi^-n \rangle = A(\frac{3}{2}) \tag{6.7.9}$$

Similarly on looking up the Clebsch–Gordan coefficients we find

$$\left. \begin{aligned} \langle \pi^-p | A | \pi^-p \rangle &= \langle \pi^+n | A | \pi^+n \rangle = \frac{1}{3}A(\frac{3}{2}) + \frac{2}{3}A(\frac{1}{2}) \\ \langle \pi^0p | A | \pi^0p \rangle &= \langle \pi^0n | A | \pi^0n \rangle = \frac{2}{3}A(\frac{3}{2}) + \frac{1}{3}A(\frac{1}{2}) \\ \langle \pi^0n | A | \pi^-p \rangle &= \langle \pi^0p | A | \pi^+n \rangle = (\sqrt{2/3})A(\frac{3}{2}) - (\sqrt{2/3})A(\frac{1}{2}) \end{aligned} \right\} \tag{6.7.10}$$

So the eight different πN scattering processes are given by just two independent isospin amplitudes, $A(\frac{1}{2})$ and $A(\frac{3}{2})$.

There is at present no convincing explanation as to why nature should have chosen such a complicated symmetry structure for hadronic interactions, but it certainly works at least to a few per cent, at which level it is presumably broken by electromagnetic interactions.

We shall be particularly concerned with relations between s -channel amplitudes which arise from the exchange of particles having a definite isospin in the t channel. The t -channel process $1 + \bar{3} \rightarrow \bar{2} + 4$ can be decomposed as

$$\langle \bar{2}4 | A | 1\bar{3} \rangle = \sum_{I_t} \langle I_1, I_3, I_{1z}, I_{3z} | I_t, I_{tz} \rangle \langle I_2, I_4, I_{2z}, I_{4z} | I_t, I_{tz} \rangle^* A(I_t) \quad (6.7.11)$$

while (6.7.8) holds for s -channel isospin. The crossing relation (4.3.1) becomes for isospin amplitudes

$$A(I_s) = \sum_{I_t} M(I_s, I_t) A(I_t) \quad (6.7.12)$$

where the isospin crossing matrix $M(I_s, I_t)$ can be obtained from the Clebsch–Gordan coefficients in (6.7.8) and (6.7.11). However some care is needed with the phase conventions for isospin states and their behaviour under charge conjugation. These are discussed in some detail in Carruthers (1966). Some useful examples are quoted in table 6.3.

To illustrate how these matrices arise we consider $\pi\pi$ scattering. In terms of isospin states $|I, I_z\rangle$ we can write

$$\left. \begin{aligned} |\pi^+\pi^+\rangle &= |2, 2\rangle \\ |\pi^+\pi^-\rangle &= \left(\frac{1}{\sqrt{3}} |0, 0\rangle + \frac{1}{\sqrt{2}} |1, 0\rangle + \frac{1}{\sqrt{6}} |2, 0\rangle \right) \\ |\pi^-\pi^+\rangle &= \left(\frac{1}{\sqrt{3}} |0, 0\rangle - \frac{1}{\sqrt{2}} |1, 0\rangle + \frac{1}{\sqrt{6}} |2, 0\rangle \right) \end{aligned} \right\} \quad (6.7.13)$$

etc. so for example

$$\left. \begin{aligned} \langle \pi^+\pi^+ | A | \pi^+\pi^+ \rangle &= A(2) \\ \langle \pi^-\pi^+ | A | \pi^+\pi^- \rangle &= \frac{1}{3}A(0) - \frac{1}{2}A(1) + \frac{1}{6}A(2) \end{aligned} \right\} \quad (6.7.14)$$

Now under crossing the s -channel process $\pi^+\pi^+ \rightarrow \pi^+\pi^+$ becomes $\pi^+\pi^- \rightarrow \pi^-\pi^+$ in the t channel, and so

$$A_s(2) = \frac{1}{3}A_t(0) - \frac{1}{2}A_t(1) + \frac{1}{6}A_t(2) \quad (6.7.15)$$

which gives the bottom row of the $\pi\pi$ crossing matrix in table 6.3. The remaining elements can be deduced similarly.

b. SU(3) symmetry

As with isospin, we expect that different scattering processes will be related by SU(3) Clebsch–Gordan coefficients if strong interactions are invariant under this symmetry (see Carruthers 1966, Gourdin 1967).

Table 6.3 *Isospin crossing matrices*

<i>s</i> -Channel	<i>t</i> -Channel	$M(I_s, I_t)$
$\pi\pi \rightarrow \pi\pi$	$\bar{\pi}\pi \rightarrow \pi\bar{\pi}$	$\begin{pmatrix} \frac{1}{3} & 1 & \frac{5}{3} \\ \frac{1}{3} & \frac{1}{2} & -\frac{5}{6} \\ \frac{1}{3} & -\frac{1}{2} & \frac{1}{3} \end{pmatrix}$
$\pi N \rightarrow \pi N$	$\bar{N}N \rightarrow \pi\bar{\pi}$	$\begin{pmatrix} \sqrt{\frac{1}{3}} & 1 \\ \sqrt{\frac{1}{3}} & -\frac{1}{2} \end{pmatrix}$
$KN \rightarrow KN$	$\bar{N}N \rightarrow K\bar{K}$	$\begin{pmatrix} -\frac{1}{2} & -\frac{3}{2} \\ -\frac{1}{2} & \frac{1}{2} \end{pmatrix}$
<i>s</i> -Channel	<i>u</i> -Channel	$M(I_s, I_u)$
$\pi N \rightarrow \pi N$	$\bar{\pi}N \rightarrow \bar{\pi}N$	$\begin{pmatrix} -\frac{1}{3} & \frac{4}{3} \\ \frac{2}{3} & \frac{1}{3} \end{pmatrix}$
$KN \rightarrow KN$	$\bar{K}N \rightarrow \bar{K}N$	$\begin{pmatrix} -\frac{1}{2} & \frac{3}{2} \\ \frac{1}{2} & \frac{1}{2} \end{pmatrix}$

The particle label matters only for the isospin so π can be replaced by any $I = 1$ particle, and K, N by any $I = \frac{1}{2}$ particles.

If we label the multiplet to which a particle belongs, i.e. $\{1\}, \{8\}, \{10\}$ etc., by μ , and its quantum numbers I, I_z, Y by ν , then the state $|1, 2\rangle$ can be decomposed into irreducible representations of SU(3) by (cf. (6.7.5))

$$|\mu_1, \nu_1\rangle \otimes |\mu_2, \nu_2\rangle = \sum_{\mu, \nu} \begin{pmatrix} \mu_1 & \mu_2 & \mu \\ \nu_1 & \nu_2 & \nu \end{pmatrix} |\mu, \nu\rangle \tag{6.7.16}$$

where the bracket () denotes a Clebsch–Gordan coefficient.

The cases of greatest practical importance in view of the multiplets discussed in section 5.2 are (Carruthers 1966, Gourdin 1967)

$$\left. \begin{aligned} \{1\} \otimes \{8\} &= \{8\} \\ \{1\} \otimes \{10\} &= \{10\} \\ \{8\} \otimes \{8\} &= \{1\} \oplus \{8_s\} \oplus \{8_a\} \otimes \{10\} \oplus \{10\} \oplus \{27\} \\ \{8\} \otimes \{10\} &= \{8\} \oplus \{10\} \oplus \{27\} \oplus \{35\} \end{aligned} \right\} \tag{6.7.17}$$

(where the subscripts s and a denote symmetric ‘d-type’ and anti-symmetric ‘f-type’ $\{8\} - \{8\} - \{8\}$ couplings respectively).

Now the SU(3) Clebsch–Gordan coefficients factorize into SU(2) Clebsch–Gordan coefficients and an iso-scalar factor in the form

$$\begin{pmatrix} \mu_1 & \mu_2 & \mu \\ \nu_1 & \nu_2 & \nu \end{pmatrix} = \langle I_1, I_2, I_{1z}, I_{2z} | I, I_z \rangle \begin{pmatrix} \mu_1 & \mu_2 & \mu \\ I_1 Y_1 & I_2 Y_2 & I Y \end{pmatrix} \tag{6.7.18}$$

These are tabulated in, for example, Particle Data Group (1974). Thus for an $\{8\}$ vector meson, V , decaying into a pair of $\{8\}$ pseudo-scalars, PS, we have, in the limit of exact $SU(3)$ symmetry,

$$\left. \begin{aligned} \frac{1}{\sqrt{2}} A(\rho \rightarrow \pi\pi) &= -\frac{2}{\sqrt{2}} A(\rho \rightarrow K\bar{K}) = -\frac{2}{\sqrt{3}} A(K^* \rightarrow K\pi) \\ &= -\frac{2}{\sqrt{3}} A(K^* \rightarrow K\eta) \\ &= -\sqrt{\frac{2}{3}} \frac{1}{\cos\theta} A(\phi \rightarrow K\bar{K}) = -\sqrt{\frac{2}{3}} \frac{1}{\sin\theta} A(\omega \rightarrow K\bar{K}) \\ &= A(V \rightarrow PS + PS) \end{aligned} \right\} \quad (6.7.19)$$

(where θ is the mixing angle of (5.2.17)). However, to test such relations it is essential to take account of the very different amounts of phase space available in the different decays because of the large mass splittings due to symmetry breaking. In particular $K^* \rightarrow K\eta$ and $\omega \rightarrow K\bar{K}$ are forbidden because the resonance mass is below the threshold of the decay channel. Within the considerable uncertainties as to how best to correct for this (see for example Gourdin (1967)) the relations seem to hold reasonably well.

But it is easier to test such relations for pole exchanges in scattering amplitudes. The $SU(3)$ invariance of hadronic scattering implies that the amplitudes may depend on μ but not on ν (cf. (6.7.11)) and so for $1 + 2 \rightarrow 3 + 4$ we have

$$\langle 34 | A | 12 \rangle = \sum_{\mu, \nu} \begin{pmatrix} \mu_1 & \mu_2 & \mu \\ \nu_1 & \nu_2 & \nu \end{pmatrix} \begin{pmatrix} \mu_3 & \mu_4 & \mu \\ \nu_3 & \nu_4 & \nu \end{pmatrix}^* A(\mu) \quad (6.7.20)$$

Thus for example in processes of the type $M + B \rightarrow M' + B'$ where M, M' and B, B' are any members of the meson and baryon octets, respectively, there are just seven independent reduced amplitudes

$$A(1), A(8_{ss}), A(8_{sa}), A(8_{aa}), A(10), A(\bar{10}), A(27) \quad (6.7.21)$$

from (6.7.17) ($A(8_{as}) = A(8_{sa})$ by time reversal invariance), and all the many processes of this class are related to just these seven amplitudes by the Clebsch–Gordan coefficients of (6.7.20) (analogously to (6.7.10)).

Of course the large mass splittings invalidate these relations at low energies, but at high energies, where the external particle masses become unimportant, we can expect such relations to hold provided that care is taken in dealing with the splitting of the trajectories which are exchanged – see section 6.8*i* below. If a decomposition similar

Table 6.4 *The octet crossing matrix* ($8 \otimes 8 \rightarrow 8 \otimes 8$)
(from de Swart 1964)

	1	8_{ss}	8_{sa}	8_{as}	8_{aa}	10	$\overline{10}$	27
1	1/8	1	0	0	± 1	$\pm 5/4$	$\pm 5/4$	27/8
8_{ss}	1/8	$-3/10$	0	0	$\pm 1/2$	$\mp 1/2$	$\mp 1/2$	27/40
8_{sa}	0	0	$\pm 1/2$	1/2	0	$\sqrt{5/4}$	$-\sqrt{5/4}$	0
8_{as}	0	0	1/2	$\pm 1/2$	0	$\mp \sqrt{5/4}$	$\pm \sqrt{5/4}$	0
8_{aa}	$\pm 1/8$	$\pm 1/2$	0	0	1/2	0	0	$\mp 9/8$
$\overline{10}$	$\pm 1/8$	$\mp 2/5$	$1/\sqrt{5}$	$\mp 1/\sqrt{5}$	0	1/4	1/4	$\mp 9/40$
27	1/8	1/5	0	0	$\mp 1/3$	$\mp 1/12$	$\mp 1/12$	7/40

The upper and lower signs refer to the s - t and s - u crossing matrices, respectively. We have changed the signs of the sa and as elements in the s - t crossing matrix to conform to the usual convention for the f -type coupling for a meson to baryon-antibaryon.

to (6.7.20) is made for the t -channel process $1 + \overline{3} \rightarrow \overline{2} + 4$ as well, the crossing relation may be written (cf. (6.7.12))

$$A(\mu_s) = \sum_{\mu_t} M(\mu_s, \mu_t) A(\mu_t) \tag{6.7.22}$$

where $M(\mu_s, \mu_t)$ is the $SU(3)$ crossing matrix. A useful example of such a matrix is given in table 6.4. We shall make use of these results below.

6.8 Regge pole phenomenology

We have found that the Regge pole contribution to a t -channel helicity amplitude is given by (6.3.7), i.e.

$$A_{H,\lambda}^R(s, t) = -16\pi(-1)^\Lambda K_{\lambda\lambda'}(t) \gamma_\lambda(t) \gamma_{\lambda'}(t) \times (e^{-i\pi(\alpha-v)} + \mathcal{S}) f_H(\alpha) \left(\frac{s-u}{2s_0}\right)^{\alpha-M} \xi_{\lambda\lambda'}(z_t) \tag{6.8.1}$$

Here $K_{\lambda\lambda'}(t)$ given in table 6.1 depends on whether or not there is a conspiracy, and $f_H(\alpha)$ depends on whether the trajectory chooses sense, nonsense etc., as discussed in section 6.3. \mathcal{A} is defined in (B.10), and $\xi_{\lambda\lambda'}(z_t)$ in (B.11). Alternatively one can work with s -channel helicity amplitudes and use (6.4.9) instead. And since Regge poles have definite values of I, S etc., there should be $SU(2)$ or $SU(3)$ relations between their contributions to the various processes connected by these internal symmetries, as discussed in the previous section. This

section contains a brief survey of how well these predictions compare with experiment. A bibliography of the large amount of detailed work on Regge predictions for individual process may be found in Collins and Gault (1975).

a. Regge behaviour

Equation (6.8.1) predicts that with a single Regge pole exchange all the helicity amplitudes for a process will have the asymptotic behaviour

$$A_H(s, t) \sim \left(\frac{s-u}{2s_0}\right)^{\alpha(t)} \sim \left(\frac{s}{s_0}\right)^{\alpha(t)} \quad (6.8.2)$$

for $s \rightarrow \infty$, t fixed, and so from (4.2.5) or (4.3.12)

$$\frac{d\sigma}{dt} \rightarrow F(t) \left(\frac{s}{s_0}\right)^{2\alpha(t)-2} \quad (6.8.3)$$

where $F(t)$ is some function of t , and from (4.2.6)

$$\sigma_{12}^{\text{tot}}(s) \sim \left(\frac{s}{s_0}\right)^{\alpha(0)-1} \quad (6.8.4)$$

so both the differential and total cross-sections should have simple power behaviours.

These expressions are valid to leading order in s/s_0 and corrections of order $(s/s_0)^{\alpha(t)-1}$ may be anticipated due to other terms in the expansion of $e_{\lambda\lambda'}^{-\alpha}(z_t)$, daughter trajectories, threshold corrections etc. So this prediction of Regge theory should hold for $s \gg s_0$, where s_0 is the scale factor which was introduced in (6.2.9). Obviously if s_0 were very large these predictions would be untestable. We cannot really deduce what s_0 should be (see however section 7.4 below) but empirically it seems to be about 1 GeV^2 , consistent with the hadronic mass scale, and so Regge theory usually works quite well for $s > 10 \text{ GeV}^2$, or (from (1.7.30)) $p_L > 5 \text{ GeV}$ for a proton target, i.e. for all energies above the resonance region. Taking $s_0 = 1 \text{ GeV}^2$ has the advantage that it can be omitted from the equations, but if so its implicit occurrence should be kept in mind.

b. The Pomeron

The total cross-sections for various states are plotted in fig. 6.4 and it will be observed that though in several cases there is a fall at low energies, and a slow rise at high energies, taken over all they are remarkably constant over a large range of s . From (6.8.4), constancy

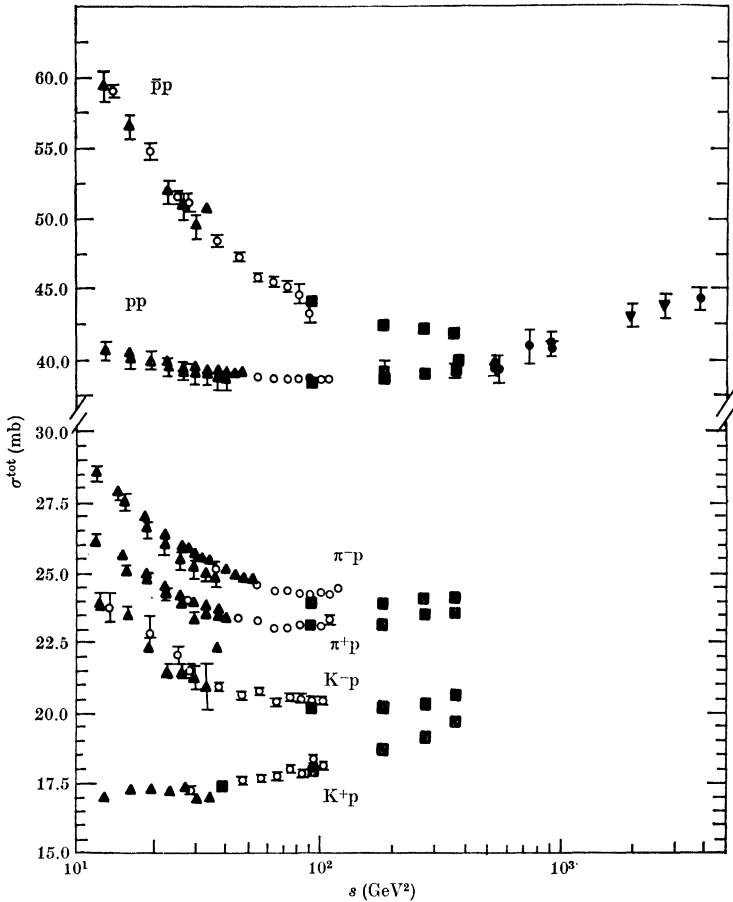


FIG. 6.4 The total cross-sections for various states as a function of s , from Barger (1974). (Note that the s scale is logarithmic.)

of $\sigma^{\text{tot}}(s)$ requires $\alpha(0) \approx 1$, but all the trajectories of figs. 5.4, 5.5 have $\alpha(0) \lesssim \frac{1}{2}$. In elastic scattering $1 + 2 \rightarrow 1 + 2$ the t channel consists of a particle and its anti-particle ($1 + \bar{1} \rightarrow \bar{2} + 2$) and so the exchanged trajectories must obviously have the quantum numbers of the vacuum (i.e. $B = Q = S = I = 0$, $P = G = C_n = \mathcal{S} = +1$). The f meson has these quantum numbers, but, at least as drawn in fig. 5.5 (a), its trajectory is much too low at $t = 0$ to explain the behaviour of the total cross-sections.

This difficulty was realised rather early in the history of Regge phenomenology, and a new trajectory called the Pomeron (or Pomeranchon or Pomeranchukon by some authors), P , with $\alpha_P(0) \approx 1$ was

invented (Chew and Frautschi 1961) to account for the asymptotic behaviour of the σ^{tot} s. Since it has even signature there is no pole near $t = 0$ because $\alpha_P(0) = 1$ is a wrong-signature point. Even signature means that its contribution is symmetric under the interchange $z_t \leftrightarrow -z_t$, i.e. $s \leftrightarrow u$ at fixed t (see (2.5.3), (2.5.6)). Now the u -channel process is $\bar{1} + 2 \rightarrow \bar{1} + 2$, and so the P-exchange hypothesis demands that $\sigma_{12}^{\text{tot}}(s) \rightarrow \sigma_{\bar{1}2}^{\text{tot}}(s)$ as $s \rightarrow \infty$, and in fig. 6.4 we see that it is quite likely that $\sigma_{pp}^{\text{tot}} \rightarrow \sigma_{\bar{p}p}^{\text{tot}}$, $\sigma_{K^+p}^{\text{tot}} \rightarrow \sigma_{K^-p}^{\text{tot}}$, $\sigma_{\pi^+p}^{\text{tot}} \rightarrow \sigma_{\pi^-p}^{\text{tot}}$ as $s \rightarrow \infty$. Such an equality was predicted on more general grounds by Pomeranchuk (1958) which accounts for the name now given to this trajectory. (See Eden (1971) for a discussion of the status of Pomeranchuk's theorem.)

Of course $\alpha_P(0) = 1$ is the maximum value permitted by the Froissart bound (2.4.10), so to have a trajectory as high as this implies that the strong interaction is as strong as it can be under crossing – i.e. unitarity is ‘saturated’. It is clearly rather unsatisfactory that we have been forced to invent a trajectory which does not seem to have any particles lying on it. However, we shall find below (fig. 6.6f) that its slope appears to be rather small, $\alpha'_P \approx 0.2 \text{ GeV}^{-2}$, so that a particle at $\alpha(t) = 2$ would have a rather high mass ($m^2 \approx 5 \text{ GeV}^2$). In any case the fact that the observed σ^{tot} s are still rising at CERN-ISR energies (which would naïvely imply $\alpha_P(0) > 1$) and the complications of Pomeron cuts (see section 8.6) make one wonder if the Pomeron may not be a more complicated singularity than a pole.

The Pomeron can be exchanged not only in elastic scattering processes but also in so-called quasi-elastic processes $1 + 2 \rightarrow 3 + 4$ where **3** has the same internal quantum numbers as **1**, and **4** has the same as **2** – for example $\pi N \rightarrow \pi N^*(\frac{1}{2})$ where $N^*(\frac{1}{2})$ is an $I = \frac{1}{2}$ baryon resonance – and so all such processes should have essentially constant high energy cross-sections. There are however, some empirical rules which restrict P-couplings.

In elastic scattering processes the P appears to couple only to the s -channel helicity-non-flip baryon vertex, and hence for example to A_{++}^s but not A_{+-}^s in $\pi N \rightarrow \pi N$ (see (4.3.10)). It is also found that in quasi-elastic processes such as $\gamma N \rightarrow \rho^0 N$, $\gamma N \rightarrow \omega N$, $\gamma N \rightarrow \phi N$, $\pi N \rightarrow \pi N^*(\frac{1}{2})$ and $NN \rightarrow NN^*(\frac{1}{2})$ there is at least approximate s -channel helicity conservation (i.e. $\mu_1 = \mu_3$, $\mu_2 = \mu_4$). It is of course rather odd that a t -channel exchange should have such simple s -channel helicity couplings. But the rule seems to be violated in $\pi N \rightarrow A_1 N$, $\pi N \rightarrow A_3 N$ and $KN \rightarrow QN$ (see for example Leith (1973) for a review).

Another empirical rule is the so-called Gribov–Morrison rule (Gribov 1967, Morrison 1967) that the Pomeron couples to a vertex, $1\bar{3}$, only if

$$(-1)^{\sigma_1 - \sigma_3} = \eta_1 \eta_{\bar{3}} \tag{6.8.5}$$

i.e. the change of spin at the vertex must be related to the change of intrinsic parity. For spinless particles ($\sigma_1 = \sigma_3 = 0$) this rule follows from parity conservation and (4.6.8), i.e. $P = \mathcal{S}\eta$. Since the Pomeron has $P = \mathcal{S} = \eta = +1$ the $1\bar{3}$ state must have

$$P = (+1) = \eta_1 \eta_{\bar{3}} (-1)^l = \eta_1 \eta_{\bar{3}} (-1)^J = \eta_1 \eta_{\bar{3}} \mathcal{S} = \eta_1 \eta_{\bar{3}} \tag{6.8.6}$$

However, for particles with spin, J is not necessarily equal to l , so there will always exist helicity states having the signature and parity of the Pomeron. But if (6.8.5) is to be violated there must be a change of helicity, and so, from (6.4.2), the Pomeron-exchange amplitudes will vanish in the forward direction.

In fact the rule often seems to apply for particles with spin (see for example Leith 1973). Thus in $\pi N \rightarrow \pi N^* \rightarrow \pi\pi N$, it is found that the N^* 's produced have $L_{21, 2S} (I \equiv \text{isospin}, S \equiv \text{spin}) = P_{11}, D_{13}, F_{15}$, with no sign of D_{15} which would violate (6.8.5). Similarly, while $\pi N \rightarrow A_1 N$, $KN \rightarrow QN$, $\gamma N \rightarrow \rho^0 N$ all seem to exhibit a Pomeron-like constant high energy cross-section, $\pi N \rightarrow A_2 N$, $KN \rightarrow K^* N$, $\gamma N \rightarrow BN$, which violate the rule, decrease with energy. However, the difficulty of making a clean separation of the resonances from background events, and the fact that secondary trajectories may produce a decrease of $\sigma(s)$ at low s anyway, make the rule hard to test decisively, and its status is still unclear.

c. The leading trajectories

If several trajectories can be exchanged in a given process then the trajectory with the highest $\text{Re}\{\alpha(t)\}$ will dominate asymptotically at any given t . How high in s one has to go before a single trajectory exchange gives a satisfactory approximation to the amplitude clearly depends on the separation of the trajectories, the relative strengths of their residues, and of course on s_0 .

So for a given process all one has to do is work out the possible quantum numbers which can occur in the t channel, and look up the leading trajectory with those quantum numbers in figs. 5.4–5.6. Table 6.5 lists the leading trajectories for most of the experimentally accessible processes.

For processes where the t -channel quantum numbers are $B = S = 0$, if charge is exchanged, or if there is a change of isospin at one of the

Table 6.5 *Regge trajectory exchanges for various processes*

Exchanges	Exchanged quantum numbers				Processes
	B	S	$(I)^G$	ηC_n	
<i>π^\pm beams</i>					
ρ	0	0	$(1)^+$	+	$\pi^-p \rightarrow \pi^0n$ $\pi^+p \rightarrow \pi^0\Delta^{++}$
A_2	0	0	$(1)^-$	+	$\pi^-p \rightarrow \eta n$ $\pi^+p \rightarrow \eta\Delta^{++}$
ρ, B	0	0	$(1)^+$	\pm	$\pi^-p \rightarrow \omega n$ $\pi^+p \rightarrow A_2^0\Delta^{++}$ $\pi^+p \rightarrow \omega\Delta^{++}$
π, A_1	0	0	$(1)^-$	-	$\pi^-p \rightarrow \varepsilon n$
A_2, π, A_1	0	0	$(1)^-$	\pm	$\pi^-p \rightarrow \rho^0n$ $\pi^-p \rightarrow fn$ $\pi^+p \rightarrow \rho^0\Delta^{++}$ $\pi^+p \rightarrow f\Delta^{++}$
ρ, f	0	0	$(0, 1)^+$	+	$\pi p \rightarrow \pi p$ $\pi p \rightarrow \pi N^*$
ρ, B, f, n, D	0	0	$(0, 1)^+$	\pm	$\pi p \rightarrow A_2 p$ $\pi p \rightarrow A_1 p$
A_2, π, A_1, ω, H	0	0	$(0, 1)^-$	\pm	$\pi p \rightarrow \rho p$ $\pi p \rightarrow B p$ $\pi p \rightarrow g p$
K^*, K^{**}	0	1	$(\frac{1}{2})$	+	$\pi^-p \rightarrow K^0\Lambda$ $\pi p \rightarrow K\Sigma$
K^*, K^{**}, K, Q	0	1	$(\frac{1}{2})$	\pm	$\pi p \rightarrow K^*\Lambda$ $\pi p \rightarrow K^*\Sigma$
N	1	0	$(\frac{1}{2})$	\pm	$\pi^-p \rightarrow n\eta$
Δ	1	0	$(\frac{3}{2})$	\pm	$\pi^-p \rightarrow p\pi^-$ $\pi^-p \rightarrow p\rho^-$
N, Δ	1	0	$(\frac{1}{2}, \frac{3}{2})$	\pm	$\pi p \rightarrow \pi p$ $\pi p \rightarrow p\rho$ $\pi p \rightarrow \Delta\pi$
Σ	1	-1	(1)	\pm	$\pi^-p \rightarrow \Lambda K^0$
Exotic					$\pi^-p \rightarrow K^+\Sigma^-$
<i>K^\pm beams</i>					
ρ, A_2	0	0	(1)	+	$K^-p \rightarrow \bar{K}^0n$ $Kp \rightarrow K\Delta$
ρ, A_2, B, π, A_1	0	0	(1)	\pm	$K^-p \rightarrow K^{*0}n$ $K^-p \rightarrow K^{**0}n$ $Kp \rightarrow K^*\Delta$
ρ, A_2, f, ω	0	0	$(0, 1)$	+	$Kp \rightarrow Kp$
$\rho, A_2, B, \pi, A_1, f, \omega, \eta, H, D$	0	0	$(0, 1)$	\pm	$Kp \rightarrow K^*p$ $Kp \rightarrow K^{**}p$ $Kp \rightarrow Qp$
K^*, K^{**}	0	1	$(\frac{1}{2})$	+	$Kp \rightarrow \pi\Lambda$ $Kp \rightarrow \pi\Sigma$ $K^-p \rightarrow \eta\Lambda$ $Kp \rightarrow \eta\Sigma$ $K^-p \rightarrow \eta'\Lambda$ $K^-p \rightarrow \pi^-\Sigma^{*+}$

Table 6.5 (cont.)

Exchanges	Exchanged quantum numbers					Processes
	B	S	$(I)^G$	η	C_n	
K^*, K^{**}, K, Q	0	1	$(\frac{1}{2})$	+		$Kp \rightarrow \rho\Lambda$ $K^-p \rightarrow \omega\Lambda$ $K^-p \rightarrow \phi\Lambda$ $Kp \rightarrow \rho\Sigma$ $K^-p \rightarrow \omega\Sigma^0$ $K^-p \rightarrow \phi\Sigma^0$
N	1	0	$(\frac{1}{2})$	\pm		$Kp \rightarrow \Lambda\pi$ $K^-p \rightarrow \Lambda n$
N, Δ	1	0	$(\frac{1}{2}, \frac{3}{2})$	\pm		$K^-n \rightarrow \Sigma^0\pi^-$
Λ, Σ	1	-1	(0, 1)	\pm		$Kp \rightarrow pK$
Exotic						$Kp \rightarrow K\Xi$
<i>p beam</i>						
ρ, A_2, B, π, A_1	0	0	(1)	\pm		$pn \rightarrow np$ $pp \rightarrow p\Delta$ $pp \rightarrow \Delta\Delta$
$\rho, A_2, B, \pi, A_1, f, \omega, \eta, H, d$	0	0	(0, 1)	\pm		$pp \rightarrow pp$
N, Δ	1	0	$(\frac{1}{2}, \frac{3}{2})$	\pm		$pp \rightarrow \pi D$ $pp \rightarrow \rho D$
<i>\bar{p} beam</i>						
ρ, A_2, B, π, A_1	0	0	(1)	\pm		$\bar{p}p \rightarrow \bar{n}n$ $\bar{p}n \rightarrow \bar{\Delta}^{++}p$ $\bar{p}p \rightarrow \Delta\Delta$
$\rho, A_2, B, \pi, A_1, f, \omega, \eta, H, D$	0	0	(0, 1)	\pm		$\bar{p}p \rightarrow \bar{p}p$
K^*, K^{**}, K, Q	0	1	$(\frac{1}{2})$	\pm		$\bar{p}p \rightarrow \bar{\Lambda}\Lambda$ $\bar{p}p \rightarrow \bar{\Lambda}\Sigma^0$ $\bar{p}p \rightarrow \bar{\Sigma}\Sigma$
N, Δ	1	0	$(\frac{1}{2}, \frac{3}{2})$	\pm		$\bar{p}p \rightarrow \pi^-\pi^+$
Λ, Σ	1	-1	(0, 1)	\pm		$\bar{p}p \rightarrow K^+K^-$
Exotic						$\bar{p}p \rightarrow \bar{\Sigma}^-\Sigma^-$
<i>Λ beam</i>						
f, ω, η, H, D	0	0	(0)	\pm		$\Lambda p \rightarrow \Lambda p$
<i>γ beam</i>						
ρ, A_2, B, π, A_1	0	0	(1)	\pm		$\gamma p \rightarrow \pi^+n$ $\gamma p \rightarrow A_1^+n$ $\gamma p \rightarrow \pi^-\Delta^{++}$
ρ, B, ω, H	0	0	(0, 1)	\pm	-	$\gamma p \rightarrow \pi^0p$ $\gamma p \rightarrow \eta p$
$A_2, \pi, A_1, f, \eta, D$	0	0	(0, 1)	\pm	+	$\gamma p \rightarrow \rho^0p$ $\gamma p \rightarrow \omega p$ $\gamma p \rightarrow \phi p$
$A_2, \pi, A_1, f, \eta, D$	0	0	(0, 1)	\pm	+	$\gamma p \rightarrow \gamma p$
K^*, K^{**}, K, Q	0	1	$(\frac{1}{2})$	\pm		$\gamma p \rightarrow K^+\Lambda$ $\gamma p \rightarrow K^{*+}\Lambda$
N	1	0	$(\frac{1}{2})$	\pm		$\gamma p \rightarrow \Delta\eta$
N, Δ	1	0	$(\frac{1}{2}, \frac{3}{2})$	\pm		$\gamma p \rightarrow n\pi^+$ $\gamma p \rightarrow p\pi^0$ $\gamma p \rightarrow \Delta^{++}\pi^-$
<i>K^0 beam</i>						
ρ, ω	0	0	(0, 1)	+	-	$K_L^0 p \rightarrow K_S^0 p$

vertices (such as $N \rightarrow \Delta$) then $I_t = 1$ only. But if there is no exchange of charge, or change of isospin at a vertex, then $I_t = 0$ or 1 . If the process has been initiated by a pion beam ($G_\pi = -1$) then the t channel will have a definite G -parity (± 1) depending on the G -parity of the final-state meson. But with K , γ or baryon beams (on a baryon target) G -parity will not be a good t -channel quantum number, and so is not restricted. If the initial state contains a pseudo-scalar particle (π or K), and the final state a pseudo-scalar, then the t channel can only contain normal parity exchanges, $\eta = +1$ (see (6.8.6)). Or more rarely if the final state contains a scalar such as ϵ then we must have abnormal parity, $\eta = -1$, exchanges. But for other spin combinations the normality is not restricted. With the neutral γ or K_L^0 beams the G -parity is not restricted, and $I_t = 0$ or 1 , but if the final state contains a neutral meson then the t channel has a definite value of $C_n (= \pm 1)$. Otherwise, C_n is not restricted.

With S and/or $B \neq 0$ exchanges, G and C_n are not restricted, so the rules are much easier to apply.

The simplest set of processes are meson-baryon charge-exchange scattering such as $\pi^- p \rightarrow \pi^0 n$. Since the t -channel $\pi^- \pi^0 \rightarrow \bar{p} n$ has charge, only $I = 1$ non-strange mesons can contribute, and the π - π vertex is restricted to even G -parity and normal parity. Only the ρ satisfies all these requirements. Similar remarks apply to $\pi^- p \rightarrow \eta n$ except that η has even G -parity and so only A_2 can be exchanged. However, in most processes the exchanges are not so simple. Thus in $K^- p \rightarrow \bar{K}^0 n$ the K mesons are not eigenstates of G -parity so both ρ and A_2 can be exchanged, and if the mesons have non-zero spin, as in $\pi^- p \rightarrow \rho^0 n$, the normality is not restricted so π exchange is allowed as well as A_2 .

Bearing the above rules in mind the reader should have no difficulty in checking table 6.5. However, these are only the leading trajectories with the given quantum numbers, and secondary or daughter ρ' , A_2' may also occur, as well as Regge cuts. (For f read f and P .)

The appearance of a Regge pole in the t (or u channel) should result in a peak of the differential cross-section near the forward (or backward) direction. An example shown in fig. 6.5 is the data for $K^+ p$ elastic scattering. Near the forward direction we see the effect of the t -channel poles, P , f , ω , ρ and A_2 , while the u channel of $K^+ p$ has the quantum numbers of the Λ and Σ baryons and so there is a smaller backward peak. However, the u channel of $K^- p \rightarrow K^- p$ is $K^+ p \rightarrow K^+ p$, which has exotic quantum numbers, and so there are no Reggeons

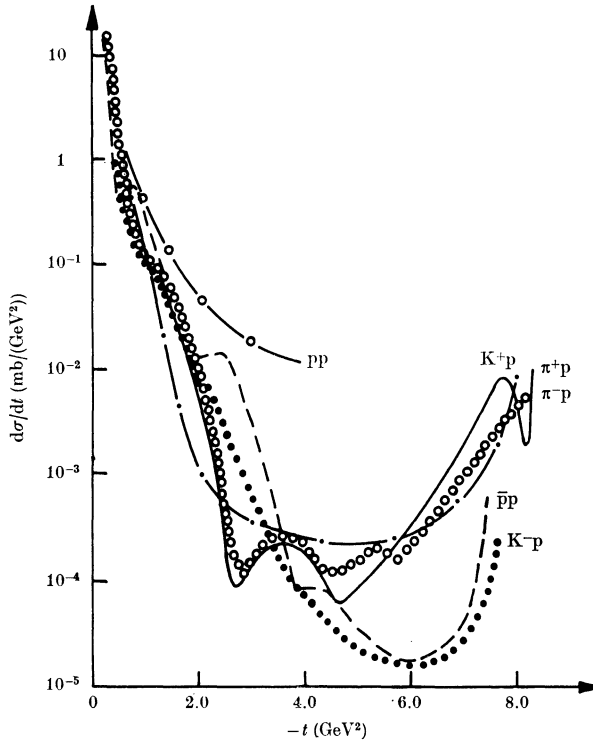


FIG. 6.5 The differential cross-sections for various elastic scattering processes at 5 GeV/c.

which can be exchanged (unless the conjectured Z particle exists – see Particle Data Group (1974)), and as expected the backward peak is strongly suppressed.

This sort of correlation between the occurrence of forward or backward peaks of $d\sigma/dt$, and the presence of non-exotic quantum numbers (and hence known trajectories) in the crossed channel, provides an excellent confirmation that particle exchange is the mediator of the strong interaction.

d. The effective trajectory

From (6.8.3)
$$\log \left(\frac{d\sigma}{dt} \right) = (2\alpha(t) - 2) \log \left(\frac{s}{s_0} \right) + \log (F(t)) \tag{6.8.7}$$

and so by plotting $\log(d\sigma/dt)$ for a given process against $\log s$, at fixed t , we can determine the ‘effective trajectory’ for that process. At sufficiently high energy this effective trajectory should correspond to the leading trajectory for the process (apart from any complications

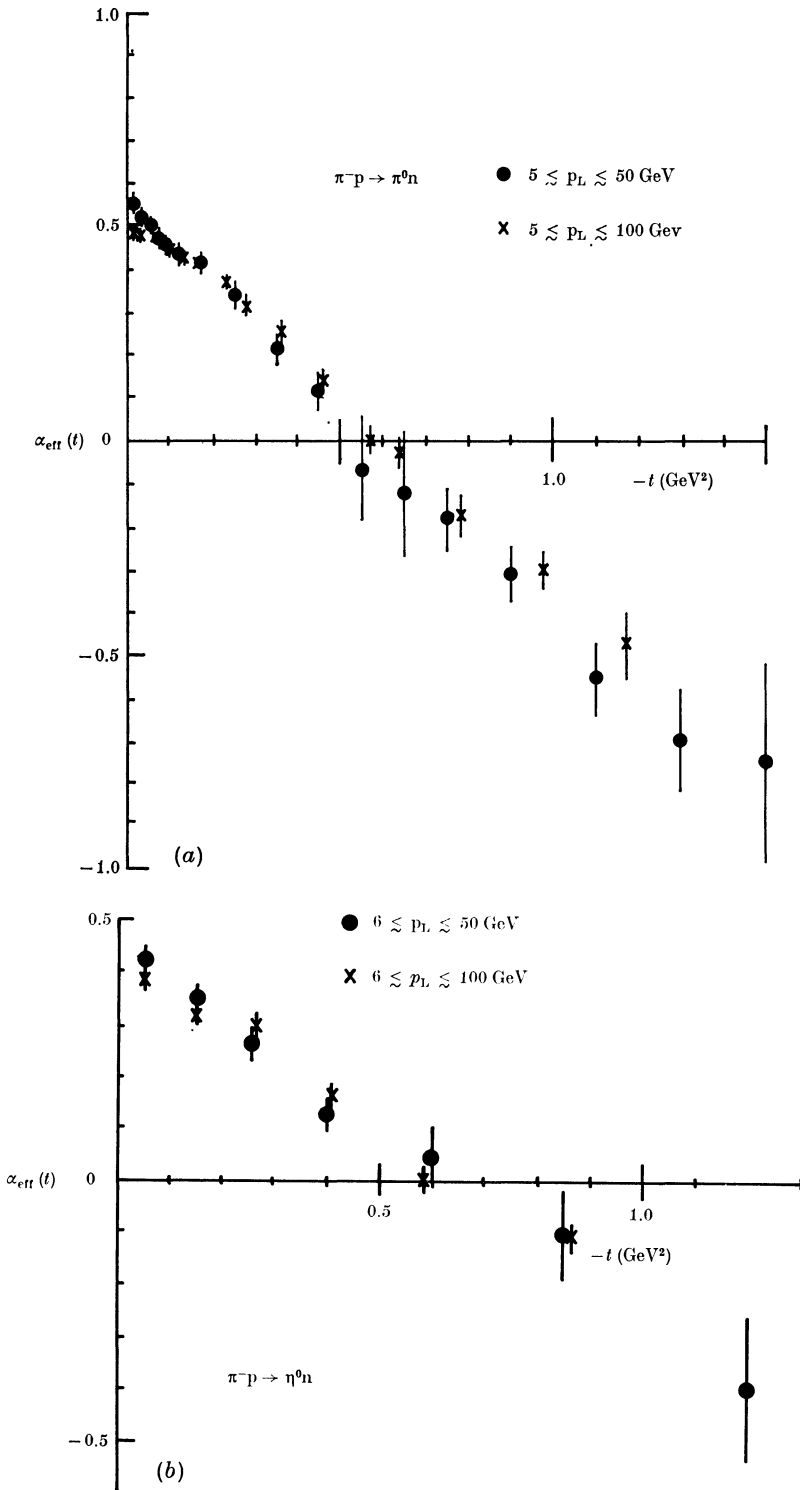


FIG. 6.6 (a), (b)

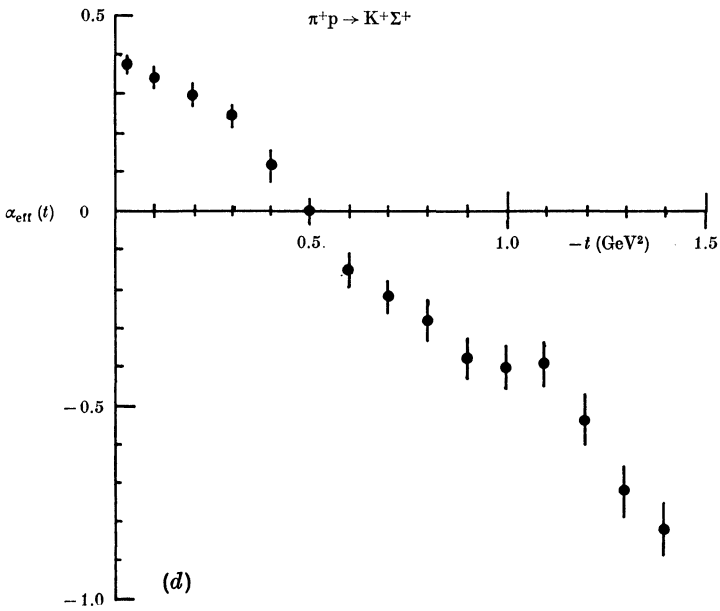
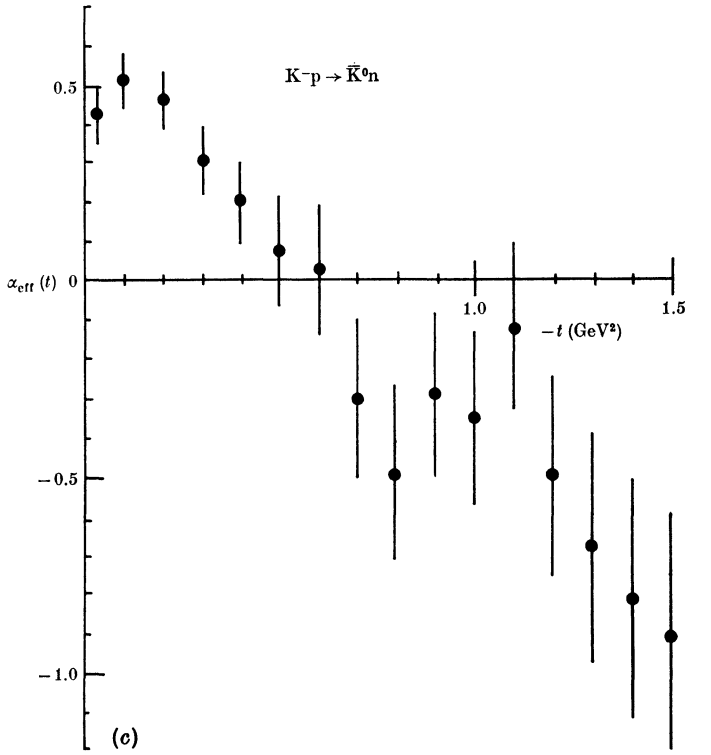


FIG. 6.6 (c), (d)

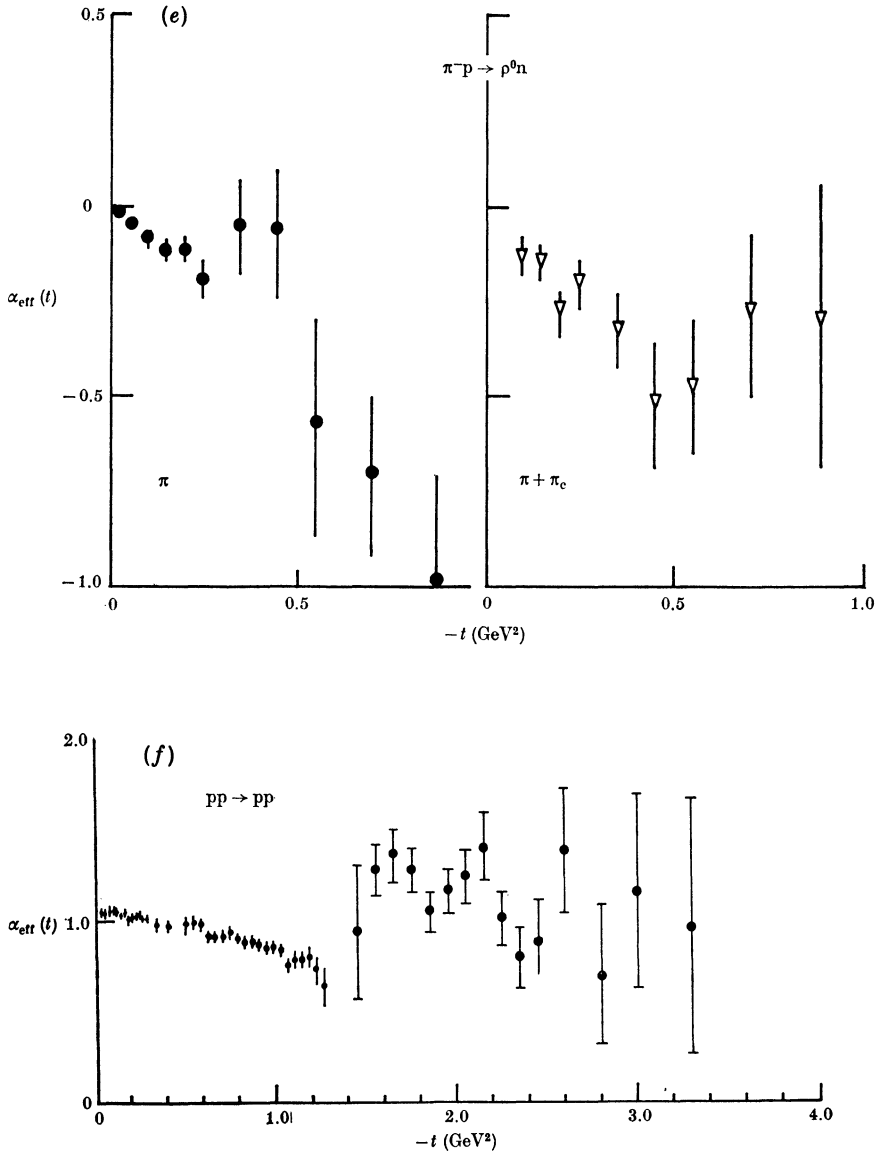


FIG. 6.6 (a)-(f) The effective trajectories for a variety of processes obtained using (6.8.7). The trajectories are: (a) ρ exchange, (b) A_2 exchange, (c) $\rho + A_2$ exchange, (d) $K^* + K^{**}$ exchange, (e) π exchange, (f) P exchange.

due to Regge cuts etc., see chapter 8 below). In fig. 6.6 we show the effective trajectory obtained from (6.8.7) for some of the processes for which there is good high energy data, and where there is reason to believe that a single trajectory may suffice.

Evidently within the experimental errors these effective trajectories are consistent with straight lines, and agree quite well with those obtained from the resonance masses in figs. 5.4 and 5.5. This is a remarkable success for Regge theory. Indeed it seems almost too good given that one might have expected curved trajectories and interference from cuts!

We noted in section 2.8 that an elementary-particle exchange would give rise to a fixed power behaviour, $A \sim s^\sigma$, where σ is the spin of the particle, independent of t . Such fixed powers are not seen, even for the exchange of stable particles such as the pion and nucleon which once seemed the best candidates for this elementary status. It thus seems safe to conclude that all hadrons are Reggeons, i.e. lie on Regge trajectories.

Also shown in fig. 6.6 (*f*) is the effective trajectory of the P obtained from high energy pp elastic scattering. It is found that

$$\alpha_P^{\text{eff}}(t) \simeq 1.08 + 0.2t \tag{6.8.8}$$

for $|t| < 1.4 \text{ GeV}^2$, i.e. the trajectory has a small slope but an intercept above 1, apparently in violation of the Froissart bound. We shall discuss this problem further in section 8.7*a*.

e. Shrinkage

Since $d\sigma/dt$ seems to fall roughly exponentially for small $|t|$ in many processes (see for example fig. 6.5) we can approximate the residue by an exponential, so that (6.8.1) becomes

$$A(s, t) \approx G e^{at} \left(\frac{s}{s_0}\right)^{\alpha(t)} \tag{6.8.9}$$

and with an approximately linear trajectory

$$\alpha(t) = \alpha^0 + \alpha't \tag{6.8.10}$$

this gives
$$A(s, t) \approx G \left(\frac{s}{s_0}\right)^{\alpha^0} e^{(a+\alpha' \log(s/s_0))t} \tag{6.8.11}$$

So if we define the ‘width’ of forward peak in t by

$$\Delta t \equiv \left(\frac{d}{dt} \left(\frac{d\sigma}{dt}\right) / \frac{d\sigma}{dt}\right)^{-1}$$

we find
$$\Delta t = [2(a + \alpha' \log s/s_0)]^{-1} \tag{6.8.12}$$

(from (6.8.11) in (4.3.12)). So Δt decreases as $\log s$ increases, i.e. Regge theory predicts that the width of the forward peak will ‘shrink’ as s increases. This effect can be detected by a close examination of fig. 6.1 in which the low energy data has a somewhat broader peak than the high energy (at small t). It is this shrinkage which produces the slopes of the effective trajectories in figs. 6.6.

From our discussion in section 2.4, one can interpret this shrinkage as an increase in the effective size of the target, but as the cross-section does not increase the target is evidently becoming more ‘transparent’ as the energy increases. Though these predictions of Regge theory once seemed rather surprising from an ‘optical’ point of view they are now well verified in a great variety of processes.

With $\alpha_P(0) = 1$ we obtain for the elastic differential cross-section from (6.8.11) and (1.8.16)

$$\left(\frac{d\sigma}{dt}\right)^{\text{el}} \rightarrow \frac{1}{16\pi} G_P^2 e^{2[a+\alpha_P' \log(s/s_0)t]}$$

and so
$$\sigma_{12}^{\text{el}}(s) = \int_{-\infty}^0 \left(\frac{d\sigma}{dt}\right) dt \rightarrow \frac{1}{16\pi} \frac{G_P^2}{2[a + \alpha_P' \log(s/s_0)t]} \tag{6.8.13}$$

while from (1.9.6) $\sigma_{12}^{\text{tot}}(s) \rightarrow G_P$, and hence $\sigma_{12}^{\text{el}}/\sigma_{12}^{\text{tot}} \sim (\log s)^{-1}$. So because of the shrinkage the elastic cross-section becomes a decreasing fraction of the total cross-section as $\log s \rightarrow \infty$.

f. The phase-energy relation

As the trajectory and residue functions are expected to be real below threshold (except where trajectories collide – see section 3.2) the phase of the Regge pole amplitude (6.8.1) is given entirely by the signature factor ($e^{-i\pi(\alpha(t)-v)} + \mathcal{S}$) and so the phase angle, ϕ , is related to the energy dependence $\alpha(s)$ by

$$\cot \phi \equiv \frac{\text{Re}\{A\}}{\text{Im}\{A\}} \equiv \rho = -\frac{\cos \pi(\alpha(t) - v) + \mathcal{S}}{\sin \pi(\alpha(t) - v)} \tag{6.8.14}$$

It is often convenient to rewrite the signature factor as (for $v = 0$)

$$\begin{aligned} e^{-i\pi\alpha} + \mathcal{S} &= e^{-i\pi\alpha/2} (e^{-i\pi\alpha/2} + \mathcal{S} e^{i\pi\alpha/2}) \\ &= e^{-i\pi\alpha/2} 2 \cos\left(\frac{\pi\alpha}{2}\right) \quad \text{for } \mathcal{S} = +1 \\ &= -i e^{-i\pi\alpha/2} 2 \sin\left(\frac{\pi\alpha}{2}\right) \quad \text{for } \mathcal{S} = -1 \end{aligned} \tag{6.8.15}$$

which exhibits this phase directly.

It is possible to determine the phase of helicity-non-flip elastic scattering amplitudes at $t = 0$, either by measuring

$$\sigma_{12}^{\text{tot}}(s) \propto \text{Im} \{A_{12}^{\text{el}}(s, 0)\}$$

and
$$d\sigma/dt (12 \rightarrow 12) \propto \text{Re} \{A_{12}^{\text{el}}\}^2 + \text{Im} \{A_{12}^{\text{el}}\}^2$$

(but $d\sigma/dt$ has to be extrapolated to $t = 0$ from the finite negative values at which it can be measured), or by observing the interference between the hadronic scattering amplitude and the known Coulomb scattering amplitude (see for example Eden (1967)). In fig. 6.7 we show the data on the ratio ρ at $t = 0$ for pp elastic scattering compared with the predictions of a Regge pole fit (Collins, Gault and Martin 1974) to $\sigma_{\text{tot}}(\text{pp})$ and $\sigma_{\text{tot}}(\overline{\text{pp}})$ using just the dominant P, f and ω trajectories (with $\alpha_{\text{P}}(0) > 1$) and evidently the agreement is quite good.

However, this is not really a test of Regge theory so much as of the power behaviour of $\text{Im} \{A_{12}^{\text{el}}\}$ and dispersion relations. Thus, for example, if we write a once-subtracted dispersion relation for the amplitude for s above threshold (from (1.10.7))

$$\text{Re} \{A(s, t)\} = \frac{s}{\pi} P \int_{s_{\text{T}}}^{\infty} \frac{\text{Im} \{A(s', t)\}}{(s' - s)s'} ds' + \frac{s}{\pi} \int_{u_{\text{T}}}^{-\infty} \frac{\text{Im} \{A(s', t)\}}{(s' - s)s'} ds' \tag{6.8.16}$$

(where $P \equiv$ principal value) and if $\text{Im} \{A(s, t)\} \underset{s \rightarrow \infty}{\sim} s^{\alpha(t)}$ and $\underset{s \rightarrow -\infty}{\sim} (-s)^{\alpha(t)}$

then since (Erdelyi *et al.* 1953)

$$\left. \begin{aligned} \frac{P}{\pi} \int_0^{\infty} \frac{ds'}{s' - s} s'^{\alpha - 1} &= -s^{\alpha - 1} \cot(\pi\alpha) \\ \frac{1}{\pi} \int_0^{\infty} \frac{ds'}{s' + s} s'^{\alpha - 1} &= -s^{\alpha - 1} \text{cosec}(\pi(\alpha - 1)) \end{aligned} \right\} \tag{6.8.17}$$

(6.8.16) gives for $s \rightarrow \infty$

$$\frac{\text{Re} \{A(s, t)\}}{\text{Im} \{A(s, t)\}} \sim -(\cot(\pi\alpha) + \mathcal{S} \text{cosec}(\pi\alpha)) \tag{6.8.18}$$

in agreement with (6.8.14) (for $v = 0$). This result holds for any number of subtractions. It is clear from (6.8.17) that where $\alpha_{\text{eff}} < 1$ we can expect $\rho < 0$, but where the cross-section rises, so $\alpha_{\text{eff}} > 1$, ρ should become positive which is indeed the case in fig. 6.7.

In general the absolute phases of scattering amplitudes cannot be determined experimentally, but the relative phases of different

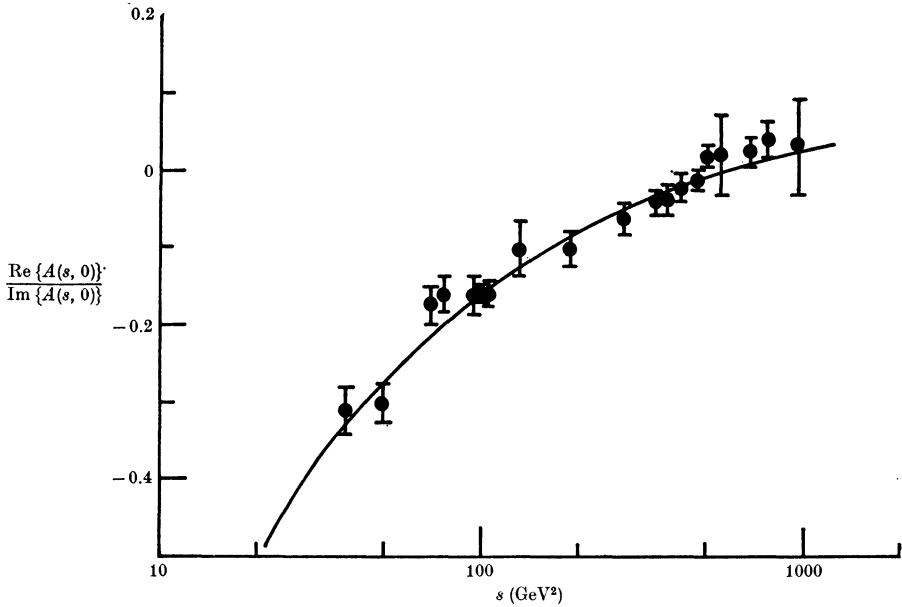


FIG. 6.7 Data on $\text{Re}\{A(s, 0)\}/\text{Im}\{A(s, 0)\}$ for pp scattering compared with the Regge pole fit of Collins *et al.* (1974).

amplitudes can be obtained. For example in $\pi^-p \rightarrow \pi^0n$ the polarization is given by (4.2.22), and so depends on the phase difference between the helicity-flip and non-flip amplitudes. A single ρ pole gives the same phase (6.8.14) (with $\nu = 0, \mathcal{S} = -1$) to both amplitudes and so ρ exchange predicts that the polarization will vanish. In fact it is observed to be small but not zero ($\approx 10\text{--}20$ per cent) at low energies (< 10 GeV) indicating the need for some other contribution in addition to the ρ pole, perhaps a cut or a secondary ρ' trajectory.

We shall discuss further examples of Regge phase predictions below.

g. Factorization and line reversal

The disconnectedness of the S -matrix leads us to expect that Regge pole residues will factorize into a contribution to each vertex (see (4.7.15)) so that for a t -channel Regge pole (fig. 6.8)

$$\beta_{12 \rightarrow 34}^R(t) = \beta_{13}^R(t) \beta_{24}^R(t) \tag{6.8.19}$$

We have found in sections 6.2 and 6.3 that this relation puts important constraints on the residues of helicity amplitudes, and it is built into (6.8.1).

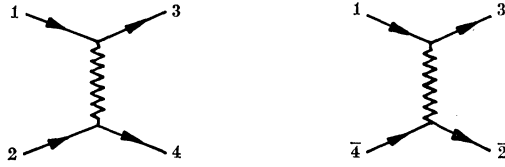


FIG. 6.8 Processes connected by line reversal.

Also in processes where a single Regge trajectory dominates it leads to relations such as

$$\left(\frac{d\sigma}{dt}\right)_{12 \rightarrow 34}^2 = \left(\frac{d\sigma}{dt}\right)_{11 \rightarrow 33} \left(\frac{d\sigma}{dt}\right)_{22 \rightarrow 44} \tag{6.8.20}$$

but unfortunately it is not easy to test such relations directly because all hadronic scattering processes rely on a nucleon target. But one such relation which does seem to work quite well (Freund 1968, Bari and Razmi 1970), within the modest accuracy of the data, is

$$\frac{\frac{d\sigma}{dt} (NN \rightarrow NN)}{\frac{d\sigma}{dt} (\pi N \rightarrow \pi N)} = \frac{\frac{d\sigma}{dt} (NN \rightarrow NN^*)}{\frac{d\sigma}{dt} (\pi N \rightarrow \pi N^*)}$$

where N^* is any $I = \frac{1}{2}$ baryon resonance so that P can be exchanged. The best direct tests of factorization can be made in inclusive reactions (chapter 10) where a greater variety of vertices is available.

Another important consequence of factorization is line reversal symmetry. Clearly if one end of the exchange diagram for $1 + 2 \rightarrow 3 + 4$ is rotated as in fig. 6.8 then $s \leftrightarrow u$ and the process $1 + \bar{4} \rightarrow 3 + \bar{2}$ is obtained, which will thus have exactly the same Regge pole exchanges, with the same couplings, except that the sign will be changed for negative signature exchanges which are odd under $s \leftrightarrow u$ (see section 2.5).

For example the processes $K^-p \rightarrow \pi^- \Sigma^+$ and $\pi^+p \rightarrow K^+ \Sigma^+$ differ only by the rotation of the $K-\pi$ vertex. The only possible pole exchanges are (see table 6.5) the natural-parity strange mesons $K^*(890)$ and $K^{**}(1400)$, of which the first has spin = 1 and hence odd signature, while the second has spin = 2 and even signature. So the Regge exchanges for these processes can be written as $K^{**} \pm K^*$ respectively. Of course only the relative signs of the contributions are determined in this way, and the individual terms have phases given by (6.8.14). Similarly the elastic scattering process $\pi^-p \rightarrow \pi^-p$ differs from $\pi^+p \rightarrow \pi^+p$ only

by line reversal, so these processes have $P + f \pm \rho$ exchanges, respectively, with the same couplings. The equality of these processes as $s \rightarrow \infty$ and P dominates is just the Pomeranchuk theorem of section 6.8*b*.

There are, however, some serious failures of factorization. For example, the zero of the ρ -exchange amplitude $A_{+-}(\pi^-p \rightarrow \pi^0n)$ at $|t| \simeq 0.55 \text{ GeV}^2$, which, as we discussed in section 6.3, could be due to a nonsense factor, should also appear in $\gamma p \rightarrow \eta p$ which is similarly dominated by ρ exchange. But there is no sign of a zero in the latter process, which makes one feel that the $\pi^-p \rightarrow \pi^0n$ dip may not be a property of the ρ pole alone, but could involve cuts as well (see section 8.7*c*). Cuts do not generally have this factorization property, so the success of factorization gives some indication of the extent to which poles dominate. But of course sums of poles do not factorize either, so it is essential to isolate a single Regge exchange in making such tests.

h. Exchange degeneracy

We remarked in section 5.3 that trajectories often occur in approximately exchange-degenerate pairs, so that for example the ρ and A_2 trajectories of fig. 5.4 and fig. 6.6 look rather like a single $B = S = 0$, $I = 1$, $\eta = +1$ trajectory, with particles having $P = (-1)^J$, $C_n = (-1)^J$, $G = (-1)^{J+1}$ at every positive integer value of J . This so-called 'weak exchange degeneracy' seems to hold quite well for the leading meson exchanges (excluding the Pomeron) and for strange baryons, though it is less good for non-strange baryons. From (4.5.7) it is evident that if amplitudes of both signature contain the same trajectory then the position of the trajectory does not depend on the u -channel (or 'exchange force') discontinuity.

If the u -channel forces do not contribute to the residues of the trajectories either then they will have degenerate residues too. This is called 'strong exchange degeneracy'. The absence of the u -channel contribution seems rather surprising, but we shall find in the next chapter theoretical reasons why this may happen. In this case the trajectories must 'choose nonsense', i.e. decouple from all amplitudes at nonsense points. This may be seen by considering for example the A_2 and f trajectories which need ghost-killing factors (see section 6.3) in all their residues at $\alpha = 0$ to avoid negative m^2 particles. And if they are exchange degenerate with the ρ and ω trajectories, respectively, the latter will have zeros in their residues too, even though for them

$\alpha = 0$ is a wrong signature-point, and so they choose nonsense (see table 6.2).

This strong exchange degeneracy has the rather important consequence that if a given process is controlled by the sum of two such degenerate trajectories the amplitudes will be proportional to

$$\beta_H[(e^{-i\pi(\alpha-v)} + \mathcal{S}) + (e^{-i\pi(\alpha-v)} - \mathcal{S})] = 2\beta_H e^{-i\pi(\alpha-v)} \quad (6.8.21)$$

while if the process depends on the difference we get

$$\beta_H[(e^{-i\pi(\alpha-v)} + \mathcal{S}) - (e^{-i\pi(\alpha-v)} - \mathcal{S})] = 2\beta_H \quad (6.8.22)$$

The magnitudes in (6.8.21) and (6.8.22) are the same, but the latter is purely real, while the former has a phase which ‘rotates’ as $\alpha(t)$ changes.

This relation should obtain for pairs of trajectories connected by line reversal. Thus for example ($K^+n \rightarrow K^0p$, $K^-p \rightarrow \bar{K}^0n$) are controlled by $A_2 \pm \rho$, respectively, as are ($K^+p \rightarrow K^0\Delta^{++}$, $K^-n \rightarrow K^0\Delta^-$), while ($K^-p \rightarrow \pi^0\Lambda$, $\pi^-p \rightarrow K^0\Lambda$) and ($\bar{K}^-p \rightarrow \pi^-\Sigma^+$, $\pi^+p \rightarrow K^+\Sigma^+$) are given by $K^{**} \mp K^*$. So if strong exchange degeneracy holds we expect in each case that the first reaction of the pair will have real phase, and the second rotating phase, and that their magnitudes will be identical. The first pair seem to achieve equality above about 5 GeV, but the situation is less clear for the others (see for example Irving, Martin and Michael (1971)), partly because of uncertainties in the normalization of the data. But these relations are not expected to be exact because there must be other contributions besides these leading trajectories to explain the non-zero polarization which is observed. According to (6.8.21) and (6.8.22) all the helicity amplitudes for a given process would have the same phase, giving zero polarization.

i. Internal symmetry relations

Since we assume that the isospin SU(2) invariance of strong interactions is exact there are a large number of relations between amplitudes involving different charge states. Thus for a process such as $\pi N \rightarrow \pi\Delta$ all the different charge combinations such as $\pi^+p \rightarrow \pi^+\Delta^+$, $\pi^+p \rightarrow \pi^0\Delta^{++}$, $\pi^-p \rightarrow \pi^0\Delta^0$, etc., share the same $I_t = 1$ ρ -exchange amplitude and are equal apart from Clebsch–Gordan coefficients. It is thus useful to analyse them all together, which is why the charges are not specified in many cases in table 6.5.

Also from (6.7.9) and (6.7.10) we find

$$\langle \pi^0 n | A | \pi^- p \rangle = \frac{1}{\sqrt{2}} (\langle \pi^+ p | A | \pi^+ p \rangle - \langle \pi^- p | A | \pi^- p \rangle) \quad (6.8.23)$$

which means that the ρ exchange, which dominates the charge-exchange process, should also, via the optical theorem (4.2.6), give the energy dependence of the difference of the total cross-sections of fig. 6.4, i.e.

$$\Delta \sigma^{\text{tot}}(\pi p) \equiv \sigma_{\pi^- p}^{\text{tot}} - \sigma_{\pi^+ p}^{\text{tot}} \sim \left(\frac{s}{s_0}\right)^{\alpha_\rho(0)-1} \quad (6.8.24)$$

which is quite well satisfied, and gives a value for $\alpha_\rho(0)$ which is consistent with fig. 6.6. Similar relations, such as

$$\langle K^0 n | A | K^- p \rangle = \langle K^- p | A | K^- p \rangle - \langle K^- n | A | K^- n \rangle \quad (6.8.25)$$

can be deduced for many processes, which means that before trying to fit the elastic scattering data it is useful to obtain information about the $I_t = 1$ exchanges by analysing the charge-exchange data.

Further interesting relations stem from the approximate SU(3) invariance. Since this symmetry is badly broken for particle masses, the splitting of the exchanged trajectories often implies quite different energy dependences for SU(3) related processes. However, in some cases the trajectories are the same because of exchange degeneracy. Thus the set of charge-exchange reactions $\pi^- p \rightarrow \pi^0 n$ (ρ exchange), $\pi^- p \rightarrow \eta n$ (A_2 exchange), $K^- p \rightarrow \bar{K}^0 n$ ($A_2 + \rho$ exchange), $K^+ n \rightarrow K^0 p$ ($A_2 - \rho$) all share the same degenerate ρ - A_2 trajectory, with a common residue if strong exchange degeneracy holds. The external mesons, π , η and K , all belong to the same SU(3) octet, and so if SU(3) is exact for the residues we obtain the relation

$$\frac{d\sigma}{dt}(\pi^- p \rightarrow \pi^0 n) + 3 \frac{d\sigma}{dt}(\pi^- p \rightarrow \eta n) = \frac{d\sigma}{dt}(K^- p \rightarrow \bar{K}^0 n) + \frac{d\sigma}{dt}(K^+ n \rightarrow K^0 p) \quad (6.8.26)$$

(assuming $\eta \approx \eta_8$) which is quite well satisfied experimentally (fig. 6.9). If higher spin particles are produced it is necessary to project out particular spin density matrices to test such equalities, and for example the relation

$$\begin{aligned} \rho \frac{d\sigma}{dt}(\pi^- p \rightarrow \rho^0 n) + \rho \frac{d\sigma}{dt}(\pi^- p \rightarrow \omega^0 n) &= \rho \frac{d\sigma}{dt}(K^- p \rightarrow K^{*0} n) \\ &+ \rho \frac{d\sigma}{dt}(K^+ n \rightarrow K^{*0} p) \quad (6.8.27) \end{aligned}$$

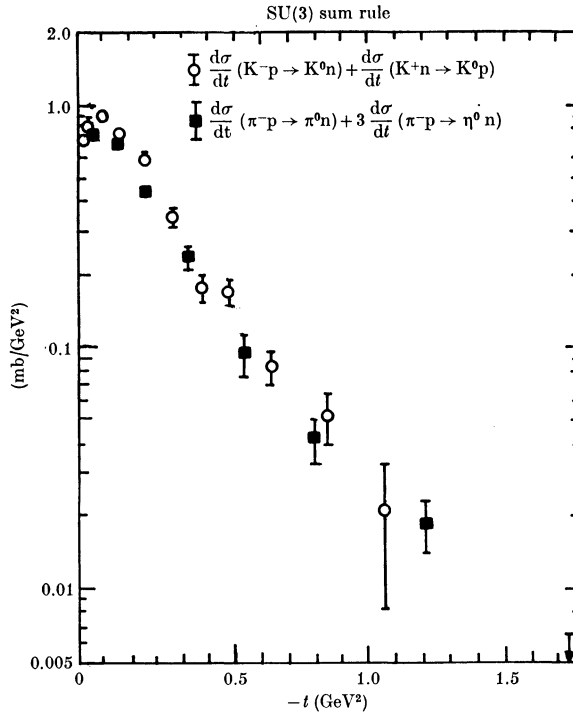


FIG. 6.9 Test of the relation (6.8.26) at 6 GeV (Barger 1974).

should work for any density matrix ρ if we assume SU(3) couplings for the vector-meson octet with ideal ω, ϕ mixing, and strong exchange degeneracy of ρ and A_2 , and again it is successful experimentally (Barger 1974).

These SU(3) predictions seem to work to about 10 per cent accuracy for all helicity amplitudes and for the differences of total cross-sections (even though one expects substantial additional contributions from Regge cuts in many processes). So SU(3) appears to be a much better symmetry for Regge couplings than it is for particle masses.

j. Forward dips and peaks

In section 6.4 we found that though an s -channel helicity amplitude has the kinematical behaviour (6.4.2) at $t = 0$, i.e.

$$A_{H_s}(s, t) \sim (-t)^{n/2} \quad \text{where} \quad n \equiv ||\mu_1 - \mu_2| - |\mu_3 - \mu_4|| \quad (6.8.28)$$

a non-conspiring t -channel Regge pole, because of factorization and

Table 6.6 Processes with dips and spikes near $t = 0$ due to π exchange

Process	Structure
$\pi^-p \rightarrow \rho^0n$	Dip
$\pi^+n \rightarrow \rho^0p$	Dip
$\pi^\pm p \rightarrow \rho^\pm p$	Dip
$\pi^+p \rightarrow \rho^0\Delta^{++}$	Spike
$\pi^+p \rightarrow f^0\Delta^{++}$	Spike
$\pi^+n \rightarrow f^0p$	Dip
$\gamma p \rightarrow \pi^+n$	Spike
$\gamma n \rightarrow \pi^-p$	Spike
$\gamma p \rightarrow \pi^-\Delta^{++}$	Dip
$\gamma n \rightarrow \pi^+\Delta^-$	Dip
$K^\pm p \rightarrow K^{*\pm}p$	Dip
$K^-p \rightarrow K^*n$	Dip
$K^\pm p \rightarrow K^*\Delta$	Spike

parity requirements, gives (6.4.7)

$$A_{H_s}(s, t) \sim (-t)^{m/2} \quad \text{where} \quad m \equiv (|\mu_1 - \mu_3| + |\mu_2 - \mu_4|) \quad (6.8.29)$$

So if we consider for example the process $\gamma p \rightarrow \pi^+n$, in which, *inter alia*, the π trajectory can be exchanged, since $\mu_\gamma = \pm 1, \mu_\pi = 0$, all the helicity amplitudes must vanish according to (6.8.29), but according to (6.8.28) the non-flip amplitudes with $|\mu_3 - \mu_4| = |\mu_1 - \mu_2|$ will not. In fact, as table 6.6 indicates, the differential cross-section has a spike in the forward direction which is of width $\Delta t \approx m_\pi^2$.

One explanation for this, which we discussed in section 6.5, is that the pion engages in a $A = 1$ conspiracy with a natural-parity trajectory. But as no such particle is observed, and as such conspiracies run into difficulties with factorization, it is generally assumed that the forward peak is due to the presence of a cut which does not have a definite t -channel parity and so is not constrained to (6.8.29) (see fig. 6.3 and section 8.7f below). Table 6.6 implies that the minimum possible helicity-flip is favoured at each vertex, i.e. at the baryon vertex $\Delta\mu \equiv \mu_2 - \mu_4 = 0$ dominates, except for the $\pi N\bar{N}$ coupling where parity conservation demands $\Delta\mu = 1$, while for meson vertices $\Delta\mu \equiv \mu_1 - \mu_3 = 0$ dominates, except that obviously for $\gamma\pi$ we can only have $\Delta\mu = \pm 1$. If these rules do not allow $n = 0$ there is a forward dip, but if $n = 0$ is permitted there is a forward spike despite (6.8.29).

Table 6.7 Processes controlled by ρ , ω and A_2 exchange

Process	Dip seen at $t \approx -0.55$?	Trajectories	n
$\pi^-p \rightarrow \pi^0n$	Yes	ρ	1
$\pi^-p \rightarrow \eta^0n$	No	A_2	1
$K^-p \rightarrow \bar{K}^0n$	No	$\rho + A_2$	1
$K^+n \rightarrow K^0p$	No	$\rho - A_2$	1
$\pi^+p \rightarrow \pi^0\Delta^{++}$	Yes?	ρ	1
$\pi^+p \rightarrow \eta\Delta^{++}$	No	A_2	1
$K^+p \rightarrow K^0\Delta^{++}$	No	$\rho - A_2$	1
$K^-n \rightarrow \bar{K}^0\Delta^-$	No	$\rho + A_2$	1
$\pi^0p \rightarrow \rho^0p$	Yes	ω	1
$\pi^\pm p \rightarrow \rho^\pm p$	Yes	$\omega + A_2$	1
$\pi^-p \rightarrow \omega n$	No	ρ	0, 2
$\pi^+n \rightarrow \omega p$	No	ρ	0, 2
$\gamma p \rightarrow \pi^0p$	Yes	$\omega(+\rho)$	1
$\gamma n \rightarrow \pi^0n$	Yes	$\omega(+\rho)$	1
$\gamma p \rightarrow \eta p$	No	$\rho(+\omega)$	0, 2
$\gamma N \rightarrow \pi^\pm N$	No	$\rho + A_2$	0, 2
$\pi^+p \rightarrow \rho^0\Delta^{++}$	No	A_2	0, 2
$K^+p \rightarrow K^*\Delta^{++}$	No?	$\rho - A_2$	0, 2
$K^-n \rightarrow \bar{K}^*\Delta^-$?	$\rho + A_2$	0, 2
$\pi^+p \rightarrow \omega\Delta^{++}$	No?	ρ	0, 2

Note: (i) We have ignored π exchange which may dominate near $t = 0$ in some of these processes. The n ($\equiv |\mu_1 - \mu_3| \pm |\mu_2 - \mu_4|$) given is relevant only to the natural-parity ρ , ω and A_2 exchanges.

(ii) We have assumed that ρ and A_2 have dominantly flip $N\bar{N}$ and $N\bar{\Delta}$ couplings, while ω is dominantly non-flip.

(iii) From $SU(3)$, $\gamma_{\omega\pi\gamma} > \gamma_{\rho\pi\gamma}$ and $\gamma_{\rho\eta\gamma} > \gamma_{\omega\eta\gamma}$.

(iv) The ρ , ω couplings to $\pi\gamma$ and πV are flip.

k. Nonsense dips

Exchange-degeneracy arguments favour nonsense-choosing couplings for Reggeons, which implies that there should be dips in various differential cross-sections where trajectories pass through wrong-signature nonsense points (see table 6.2).

The trajectories of fig. 6.6 show that the wrong-signature point $\alpha(t) = 0$ occurs for the ρ and ω trajectories at $|t| \approx 0.55 \text{ GeV}^2$. However, this point is right-signature for A_2 and f , which will give a finite contribution (but not a pole) at $\alpha(t) = 0$. Similarly $\alpha(t) = -1$, which with linear trajectories is at $|t| \approx -1.6 \text{ GeV}^2$, is right-signature for ρ , ω and wrong-signature for A_2 , f . Table 6.7 lists some of the processes which should be dominated by these trajectories (except that f is always overshadowed by P) and it is evident that many of the expected

dips occur, but by no means all. Hence either the poles do not always choose nonsense, or there are other important contributions, probably cuts, in addition to these leading trajectories, or both. Given that factorization relates the behaviour in various processes it seems to be rather hard to salvage this nonsense decoupling idea despite its apparent success in many cases.

Similar conclusions apply to other exchanges. Some of the zeros expected from other bosons, such as K^* exchange at $\alpha(t) = 0$ (i.e. $|t| \approx 0.2 \text{ GeV}^2$), and from baryons, like N exchange at $\alpha(u) = -\frac{1}{2}$ (i.e. $|u| \approx 0.2 \text{ GeV}^2$), are seen, but not all. It seems clear that cuts must play an important role, and we shall discuss this problem further in section 8.7c.

1. The cross-over problem

One rather unexpected feature of elastic differential cross-sections is that for example, $d\sigma/dt(\pi^-p \rightarrow \pi^-p) > d\sigma/dt(\pi^+p \rightarrow \pi^+p)$ for t near zero, but they become equal for $|t| \approx 0.15 \text{ GeV}^2$ and at larger $|t|$ the sign of the inequality is reversed (Ambats *et al.* 1974). From (6.8.3) and table 6.5 we see that the difference between these cross-sections is due to ρ exchange. So we can write

$$\frac{d\sigma}{dt}(\pi^\pm p) = |(P + f \mp \rho)_{++}|^2 + |(P + f \mp \rho)_{+-}|^2 \quad (6.8.30)$$

where we have dropped the kinematical factors in (4.2.5), the subscripts refer to the s -channel helicity amplitudes (4.3.10), and the Regge pole amplitudes are represented by their symbols.

It is found that the largest contribution is that of the P , which near $t = 0$ is almost purely imaginary (from $\alpha_P(0) \approx 1, \mathcal{S} = +1$ in (6.8.14)), and that P and f have at most a very small coupling to the helicity-flip amplitude, so we have

$$\frac{d\sigma}{dt}(\pi^\pm p) \approx |(P)_{++}|^2 + |(P)_{+-}|^2 \text{Im}\{(f \mp \rho)_{++}\} \quad (6.8.31)$$

so that

$$\Delta \left[\frac{d\sigma}{dt}(\pi^\pm p) \right] \equiv \frac{d\sigma}{dt}(\pi^-p \rightarrow \pi^-p) - \frac{d\sigma}{dt}(\pi^+p \rightarrow \pi^+p) \propto \text{Im}\{(\rho)_{++}\} \quad (6.8.32)$$

and hence the imaginary part of the ρ non-flip amplitude must have the 'cross-over zero' at $|t| \approx 0.15 \text{ GeV}^2$.

Similar cross-overs occur at about the same value of t in other elastic processes such as $\Delta[d\sigma/dt(K^\pm p)]$, and $d\sigma/dt(pp) - d\sigma/dt(\bar{p}p)$, as well as in some quasi-elastic processes like $\Delta[d\sigma/dt(K^\pm p \rightarrow Q^\pm p)]$, and for these processes the difference depends on $\text{Im}\{(\rho + \omega)_{++}\}$, the ω contribution being much the larger.

It is possible to fit these differential cross-sections with poles by inserting arbitrary zeros in the ρ and ω non-flip residues (see for example Barger and Phillips (1969)), but there are two difficulties. First, in other processes such as $\pi^- p \rightarrow \omega n$ (ρ exchange), $\pi^\pm p \rightarrow \rho^\pm p$ (ω and A_2 exchange) or $\gamma p \rightarrow \pi^0 p^-$ (ρ and ω), where ρ and ω are also coupled to the $p\bar{p}$ vertex, no corresponding zero is seen. In other words, the residue does not factorize. Secondly, a zero of the pole residue would imply that the real and imaginary parts of the amplitude have coincident zeros. We shall find in the next section that this is not the case. It seems clear therefore that there must be some other explanation for these zeros, and again cuts seem likely to take the blame (see section 8.7*b*).

m. The phases of amplitudes and polarization

Since a Regge pole gives the same phase to all helicity amplitudes, processes in which only a single Regge trajectory (or an exchange-degenerate pair of trajectories) is exchanged are predicted to have zero polarization (from, for example, (4.2.22)).

In fact polarization in $\Delta S = 0$ meson-baryon scattering processes is generally quite small, usually < 20 per cent (although at present the crucial $\pi^- p \rightarrow \pi^0 n$ data is contradictory on this point, cf. Bonamy *et al.* (1973) and Hill *et al.* (1973)), but the fact that it is non-zero means that there must certainly be other contributions, either lower-lying poles or cuts.

It has proved possible, by judiciously combining and interpolating data on $\pi^\pm p$ elastic scattering and $\pi^- p \rightarrow \pi^0 n$, including polarization and spin-correlation measurements, completely to determine the structure of the $\pi N \rightarrow \pi N$, $I_t = 0, 1$, A_{++} and A_{+-} amplitudes up to a common over-all phase (Halzen and Michael 1971). Since the $I_t = 0$ A_{++} amplitude should have the almost pure-imaginary phase of the Pomeron for small $|t|$ this amounts almost to a complete phase determination.

The results for $I_t = 1$ are shown in fig. 6.10. Looking first at A_{+-} , we see the forward zero required by kinematics, and the nonsense-

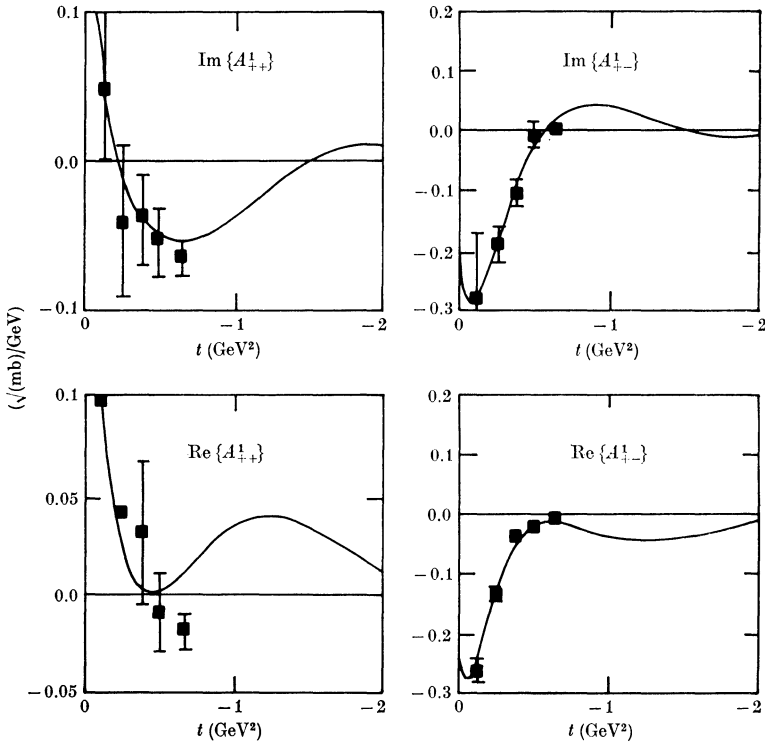


FIG. 6.10 The s -channel helicity amplitudes for $I_t = 1 \pi N$ scattering at 6 GeV, from Halzen and Michael (1971). ■ Halzen–Michael amplitude analysis; — Barger–Phillips FESR Regge analysis.

choosing phase given by

$$i e^{-\frac{1}{2}i\pi\alpha(t)}\alpha(t), \quad \alpha(t) \approx 0.5 + 0.9t \tag{6.8.33}$$

(from (6.8.15) with $\mathcal{S} = -1$), so that the imaginary part has a single zero, and the real part a double zero at $\alpha(t) = 0$, i.e. at $|t| \approx 0.55 \text{ GeV}^2$. This double zero can be seen directly in the elastic polarization since, from (4.2.22), using the same notation and approximations as led to (6.8.32),

$$\frac{d\sigma}{dt} P(\pi^\pm p \rightarrow \pi^\pm p) = \mp \text{Im} \{ (P+f)_{++}(\rho)_{+-}^* \} \approx \mp |(P)_{++}| \text{Re} \{ (\rho)_{+-} \} \tag{6.8.34}$$

since the Pomeron is nearly pure imaginary. The elastic polarization (fig. 6.11) does indeed have the mirror symmetry and double zero at $|t| \approx 0.55 \text{ GeV}^2$ predicted by (6.8.33). So the $I_t = 1, A_{+-}$ amplitude

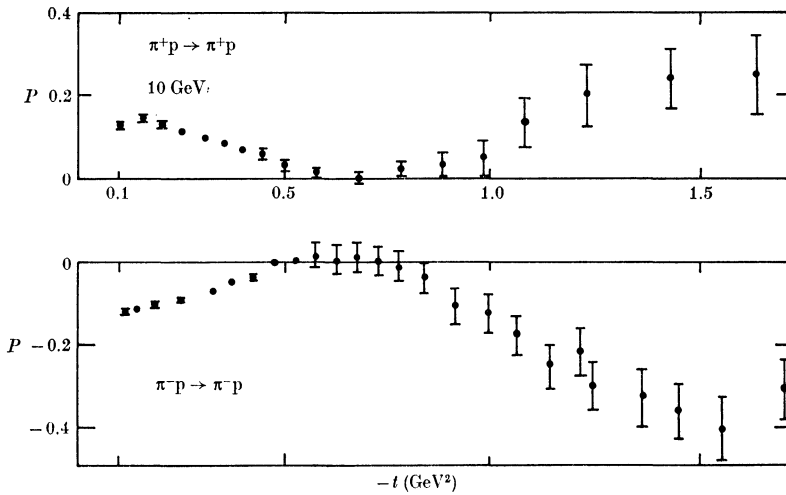


FIG. 6.11 Polarization in elastic $\pi^\pm p$ scattering, form Borghini *et al.* (1971, 1971).

can readily be parameterized by a nonsense-choosing ρ pole. The A_{++} amplitude has the cross-over zero in $\text{Im}\{A_{++}\}$ at $|t| \simeq 0.15 \text{ GeV}^2$, but the real part has what looks like a double zero at $|t| \simeq 0.55 \text{ GeV}^2$. So it seems that only $\text{Im}\{A_{++}\}$ is significantly different from what one would expect from a ρ pole.

Although at present we lack sufficient spin-dependent measurements to make similar complete amplitude decompositions for other processes, a careful use of the assumption that Regge pole phases hold good in some amplitudes has permitted quite a lot of information to be obtained about amplitude structures. Many amplitudes do seem to have approximate Regge phases, but certainly not all, and there is as yet no proper understanding of the successes and failures.